Mon. Not. R. Astron. Soc. **352,** 20–38 (2004) doi:10.1111/j.1365-2966.2004.07832.x

Measuring α in the early Universe: cosmic microwave background polarization, re-ionization and the Fisher matrix analysis

G. Rocha,[1,2⋆] R. Trotta,[3] C. J. A. P. Martins,[2,4,5] A. Melchiorri,[6,7] P. P. Avelino,[8] R. Bean[9] and P. T. P. Viana[2,10]

[1]*Astrophysics Group, Cavendish Laboratory, University of Cambridge, Madingley Road, Cambridge CB3 0HE*
[2]*Centro de Astrofísica da Universidade do Porto, R. das Estrelas s/n, Porto 4150-762, Portugal*
[3]*Département de Physique Théorique, Université de Genève, 24 quai Ernest Ansermet, CH-1211 Genève 4, Switzerland*
[4]*Department of Applied Mathematics and Theoretical Physics, Centre for Mathematical Sciences, University of Cambridge, Wilberforce Road, Cambridge CB3 0WA*
[5]*Institut d'Astrophysique de Paris, 98 bis Boulevard Arago, Paris 75014, France*
[6]*Department of Physics, Nuclear & Astrophysics Laboratory, University of Oxford, Keble Road, Oxford OX1 3RH*
[7]*Universita' di Roma 'La Sapienza', Ple Aldo Moro 2, Rome 00185, Italy*
[8]*Centro de Física do Porto e Departamento de Física da Faculdade de Ciências da Universidade do Porto, Rua do Campo Alegre 687, Porto 4169-007, Portugal*
[9]*Department of Astrophysical Sciences, Princeton University, Peyton Hall, Ivy Lane, Princeton, NJ 08544-1001, USA*
[10]*Departamento de Matemática Aplicada da Faculdade de Ciências da Universidade do Porto, Rua do Campo Alegre 687, Porto 4169-007, Portugal*

Accepted 2004 March 10. Received 2004 March 5; in original form 2003 September 10

ABSTRACT

We present a detailed analysis of present and future cosmic microwave background (CMB) constraints of the value of the fine-structure constant, α. We carry out a more detailed analysis of the *WMAP* first-year data, deriving state-of-the-art constraints on α and discussing various other issues, such as the possible hints for the running of the spectral index. We find, at 95 per cent confidence level, that $0.95 < \alpha_{\rm dec}/\alpha_0 < 1.02$. Setting $\mathrm{d}n_S/\mathrm{d}\ln k = 0$ yields $0.94 < \alpha_{\rm dec}/\alpha_0 < 1.01$ as previously reported. We find that a lower value of $\alpha_{\rm dec}/\alpha_0$ makes a value of $\mathrm{d}n_S/\mathrm{d}\ln k = 0$ more compatible with the data. We also perform a thorough Fisher matrix analysis (including both temperature and polarization, as well as α and the optical depth τ), in order to estimate how future CMB experiments will be able to constrain α and other cosmological parameters. We find that *Planck* data alone can constrain τ with an accuracy of the order 4 per cent and that this constraint can be as small as 1.7 per cent for an ideal cosmic variance limited (CVL) experiment. Constraints on α are of the order of 0.3 per cent for *Planck* and can in principle be as small as 0.1 per cent using CMB data alone: tighter constraints will require further (non-CMB) priors.

Key words: cosmic microwave background – cosmological parameters – cosmology: miscellaneous – cosmology: observations – cosmology: theory – large-scale structure of Universe.

1 INTRODUCTION

The recent release of the *Wilkinson Microwave Anisotropy Probe* (*WMAP*) first-year data (Bennett et al. 2003; Hinshaw et al. 2003; Kogut et al. 2003; Verde et al. 2003) has pushed cosmology into a new stage. On the one hand, it has quantitatively validated the broad features of the standard cosmological model – the optimistically named concordance model. At the same time, however, it has also pushed the borderline of research to new territory. We now know that dark components make up the overwhelming majority of the energy budget of the Universe. Most of this is almost certainly in some non-baryonic form, for which there is at present no direct evidence or solid theoretical explanation. One must therefore try to understand the nature of this dark energy, or at least (as a first step) look for clues of its origin.

It is clear that such an effort must be firmly grounded within fundamental physics and indeed that recent progress in fundamental physics may shed new light on this issue. On the other hand, this is not a one-way street. Cosmology and astrophysics are playing an increasingly important role as fundamental physics test-beds, because they provide us with extreme conditions (that one has no hope of reproducing in terrestrial laboratories) in which to carry out a plethora of tests and search for new paradigms. Perhaps the

⋆E-mail: graca@mrao.cam.ac.uk

more illuminating example is that of multidimensional cosmology. Currently preferred unification theories (Polchinski 1998; Damour 2003a) predict the existence of additional space–time dimensions, which will have a number of possibly observable consequences, including modifications in the gravitational laws on very large (or very small) scales (Will 2001) and space–time variations of the fundamental constants of nature (Martins 2002; Uzan 2003).

There have been a number of recent reports of evidence for a time variation of fundamental constants (Webb et al. 2001, 2003; Ivanchik et al. 2003; Murphy, Webb & Flambaum 2003) and apart from their obvious direct impact if confirmed they are also crucial in a different, indirect way. They provide us with an important (and possibly even unique) opportunity to test a number of fundamental physics models that might otherwise be untestable. A case in point is that of string theory (Polchinski 1998). Indeed here the issue is not if such a theory predicts such variations, but at what level it does so and hence if there is any hope of detecting them in the near future (or if we have done it already). Indeed, it has been argued (Damour 2003a,b). that even the results of Webb and collaborators (Webb et al. 2001, 2003; Murphy et al. 2003) may be hard to explain in the simplest, best motivated models where the variation of alpha is driven by the space–time variation of a very light scalar field. Playing the devil's advocate, one could certainly conceive that cosmological observations of this kind could one day prove string theory wrong.

The most promising case, and the one that has been the subject of most recent work (and speculation), is that of the fine-structure constant α, for which some fairly strong statistical evidence of time variation at redshifts $z \sim 2$–3 already exists (Webb et al. 2001, 2003; Murphy et al. 2003), together with weaker (and somewhat more controversial) evidence from geophysical tests using the Oklo natural nuclear reactor (Fujii 2003). Interesting and quite tight constraints can also be derived from local laboratory tests (Marion et al. 2003) and indeed this is a context where improvements of several orders of magnitude can be expected in the coming years.

On the other hand, the theoretical expectation in the simplest, best motivated model is that α should be a non-decreasing function of time (Damour & Nordtvedt 1993; Santiago, Kalligas & Wagoner 1998; Barrow, Sandvik & Magueijo 2002). This is based on rather general and simple assumptions, in particular that the cosmological dynamics of the fine-structure constant is governed by a scalar field whose behavior is akin to that of a dilaton. If this is so, then it is particularly important to try to constrain it at earlier epochs, where any variations relative to the present-day value should therefore be larger. In this regard, note that one of the interpretations of the Oklo results (Fujii 2003) is that α was larger at the Oklo epoch (effectively $z \sim 0.1$) than today, whereas the quasar results (Webb et al. 2001, 2003; Murphy et al. 2003) indicate that α was smaller at $z \sim 2$–3 than today. Both results are not necessarily incompatible, because they refer to two different cosmological epochs and hence comparing them necessarily requires specifying not only a background cosmological model but also a model for the variation of the fine-structure constant with redshift, $\alpha = \alpha(z)$. However, if both results are validated by future experiments, then the above theoretical expectation must clearly be wrong (with clear implications for both the dilaton hypothesis and on a wider scale), which would be a perfect example of using astrophysics to learn about fundamental physics.

Cosmic microwave background (CMB) anisotropies provide an ideal way of measuring the fine-structure constant at high redshift, being mostly sensitive to the epoch of decoupling, $z \sim 1100$ (one could also envisage searching for spatial variations at the last scattering surface Sigurdson, Kurylov & Kamionkowski 2003). Here we continue our ongoing work in this area (Avelino et al. 2000, 2001; Martins et al. 2002) and particularly extend our most recent analysis (Martins et al. 2004) of the *WMAP* first-year data, providing updated constraints on the value of α at decoupling, studying some crucial degeneracies with other cosmological parameters and discussing what improvements can be expected with forthcoming data sets.

We emphasize that in previous (pre-*WMAP*) work, CMB-based constraints on α were obtained with the help of additional cosmological data sets and priors. This has raised some eyebrows among skeptics, as different data sets could possibly have different systematic errors that are impossible to control and could conceivably conspire to produce the results we quoted (statistically, consistency with the value of α at decoupling being the same as today's, though with a slight preference towards smaller values). Here, by contrast, we will present results of an analysis of the *WMAP* data set alone (we will only briefly discuss what happens when other data sets are added). We also discuss how these constraints can be improved in the future, especially when more precise CMB polarization data is available. In particular, we show that the existence of an early re-ionization epoch is a significant help in further constraining α and indeed the prospects for measuring α from the CMB are much better than if the optical depth τ was much smaller.

Moreover, now that CMB polarization data is available, there are two approaches one can take. One is to treat CMB temperature and polarization as different data sets and carry out independent analyses (and, more to the point, cosmological parameter estimations), to check if the results of the two are consistent. The other one is to combine the two data sets, thus getting smaller errors on the parameters. We will show that there are advantages to both approaches and also that the combination of the two can often by itself break many of the cosmological degeneracies that plague this kind of analysis pipeline. On the other hand, we will also show that in ideal circumstances [i.e. a cosmic variance limited (CVL) experiment] CMB polarization is much better than CMB temperature in determining cosmological parameters. This result is not new and it is of course somewhat obvious, but it has never been quantified in detail as will be done below.

On the other hand, because CVL experiments are expensive and experimentalists work with limited budgets, it is important to provide detailed forecasts for future experiments. We provide detailed forecasts for the full (4-yr) *WMAP* data set, as well as for the ESA *Planck* surveyor (to be launched in 2007). It will be shown that *Planck* is almost CVL (taking into account the range of multipoles covered by this instrument) when it comes to CMB temperature, but far from it for CMB polarization. Again this was previously known, but had not been quantified. This and the intrinsic superiority of CMB polarization in measuring cosmological parameters are therefore arguments for a post-*Planck*, polarization-dedicated experiment. A longer version of this paper including tabulated results and discussion on principal directions as well as tabulated results for a small value of the optical depth, $\tau = 0.02$, can be found in the astrophysics archive with reference number astro-ph/0309211.

2 CMB TEMPERATURE AND POLARIZATION

Following Kosowsky (1996), Hu & White (1997), Zaldarriaga & Seljak (1997) and Hu (2003), one can describe the CMB anisotropy field as a 2×2, I_{ij}, intensity tensor, which is a function of direction on the sky $\boldsymbol{n}$ and two other directions perpendicular to $\hat{\boldsymbol{n}}$, which define its components $\hat{\boldsymbol{e}_1}, \hat{\boldsymbol{e}_2}$. The CMB radiation is expected to be polarized as a result of Thomson scattering of temperature

anisotropies at the time when CMB photons last scattered. Polarized light is traditionally described via the Stokes parameters, Q, U, V, where $Q = (I_{11} - I_{22})/4$ and $U = I_{12}/2$, while the temperature anisotropy is given by $T = (I_{11} + I_{22})/4$ and V can be ignored because it describes circular polarization, which cannot be generated through Thomson scattering. Both Q and U depend on the choice of coordinate system. Most of the literature on the polarization of the CMB uses three alternative representations based on either the Newman–Penrose spin-weight-2 harmonics (Zaldarriaga & Seljak 1997), or a coordinate representation of the tensor spherical harmonics (Kamionkowski, Kosowsky & Stebbins 1997a,b), or the coordinate-independent, projected symmetric trace-free (PSTF) tensor valued multipoles (Challinor 2000). Here we follow the first by expanding the polarization in the sky in terms of spin-weighted harmonics, which form a basis for tensor functions in the sky. Linear polarization can be decomposed into a curl-free part, the electric E mode, and a divergence-free part, the magnetic B mode (Seljak & Zaldarriaga 1997; Kamionkowski et al. 1997a), which are scalars under rotation. These are related to the Stokes parameters by:

$$(Q \pm \mathrm{i}U)(\hat{\boldsymbol{n}}) = \sum_{lm} (E_{lm} \mp \mathrm{i}B_{lm})_{\mp 2}\, Y_{lm}(\hat{\boldsymbol{n}}),$$

where ${}_2Y_{lm}$ are the so-called spin-2 spherical harmonics, which form a complete and orthonormal basis for spin-2 functions; and E_{lm}, B_{lm} are the the spherical multipoles on the full sky of the E and B modes, respectively. Rotational and parity invariance imply four non-zero power spectra, C_{Tl}, C_{El}, C_{Bl}, and C_{TEl}, where the power spectra C_{El} is defined by $C_{El} = \langle E_{lm} E^*_{lm} \rangle$. This E–B mode decomposition is also useful because the B mode is a direct signature of the presence of a background of gravitational waves, because it cannot be produced by density fluctuations (Zaldarriaga & Seljak 1997; Kamionkowski et al. 1997a). Many models of inflation predict a significant gravity wave background. These tensor fluctuations generated during inflation have their largest effects on large angular scales and add in quadrature to the fluctuations generated by scalar modes. Whilst recent *WMAP* results placed limits on the amplitude of these tensor modes one still lacks experimental evidence for the presence of a stochastic background of gravitational waves. As mentioned above, the detection of the pseudo-scalar field B would provide invaluable information about inflation in that they reflect the presence of such a background. Therefore to fully characterize the CMB anisotropies only four power spectra are needed: those for T, E, B and the cross-correlation between T and E. (Given that B has the opposite parity of E and T, their cross-correlations with B vanishes.)

The first detection of polarization of the CMB was as a result of the DASI experiment (Kovac et al. 2002) and more recently the *WMAP* experiment (Kogut et al. 2003) has measured the TE cross-correlation power spectrum. An important result from these is the existence of re-ionization at larger redshifts then expected from the Gunn–Petterson trough, an issue that we will discuss at length below.

3 THE CMB, α AND τ

The reason why the CMB is a good probe of variations of the fine-structure constant is that these alter the ionization history of the Universe (Hannestad 1999; Kaplinghat, Scherrer & Turner 1999; Avelino, Martins & Rocha 2000; Avelino et al. 2000). The dominant effect is a change in the redshift of recombination, as a result of a shift in the energy levels (and, in particular, the binding energy) of hydrogen. The Thomson scattering cross-section is also changed for all particles, being proportional to α^2. A smaller effect (which has so far been neglected) is expected to come from a change in the helium abundance (Trotta & Hansen 2004).

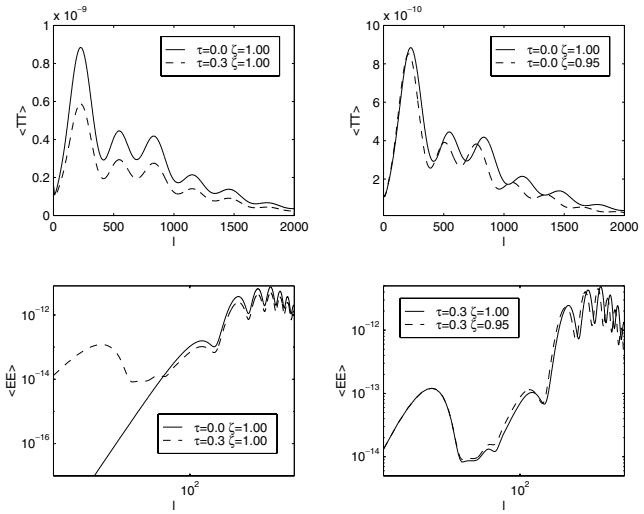

Figure 1. Contrasting the effects of varying α (right)and re-ionization (left) on the CMB temperature (top) and polarization (bottom). Here $\zeta = \alpha_{\rm dec}/\alpha_0$. See the text for further details.

Increasing α increases the redshift of last scattering, which corresponds to a smaller sound horizon. Because the position of the first Doppler peak ($\ell_{\rm peak}$) is inversely proportional to the sound horizon at last scattering, increasing α will produce a larger $\ell_{\rm peak}$ (Avelino et al. 2000). This larger redshift of last scattering also has the additional effect of producing a larger early Integrated Sachs–Wolfe (ISW) effect and hence a larger amplitude of the first Doppler peak (Hannestad 1999; Kaplinghat et al. 1999). Finally, an increase in α decreases the high-ℓ diffusion damping (which is essentially the result of the finite thickness of the last-scattering surface) and thus increases the power on very small scales. These effects have been implemented in a modified CMBFAST algorithm, which allows a varying α parameter (Avelino et al. 2000, 2001). These follow the extensive description given in Hannestad (1999) and Kaplinghat et al. (1999), with one important exception that will be discussed below.

Fig. 1 illustrates the effect of α and τ on the CMB temperature and polarization power spectra. The CMB power spectrum is, to a good approximation, insensitive to how α varies from last scattering to today. Given the existing observational constraints, one can therefore calculate the effect of a varying α in both the temperature and polarization power spectra by simply assuming two values for α, one at low redshift (effectively the value of today, because any variation of the magnitude of Webb et al. (2001) would have no noticeable effect) and one around the epoch of decoupling, which may be different from the value of today. [In earlier works, such as Hannestad (1999), Kaplinghat et al. (1999), Avelino et al. (2000) and Battye, Crittenden & Weller 2001, one assumed a constant value of α throughout, i.e. the values at re-ionization and the present day were always the same.]

For the CMB temperature, re-ionization simply changes the amplitude of the acoustic peaks, without affecting their position and spacing (top left panel); a different value of α at the last scattering, on the other hand, changes both the amplitude and the position of the peaks (top right panel).

The outstanding effect of re-ionization is to introduce a bump in the polarization spectrum at large angular scales (lower left panel). This bump is produced well after decoupling (at much lower

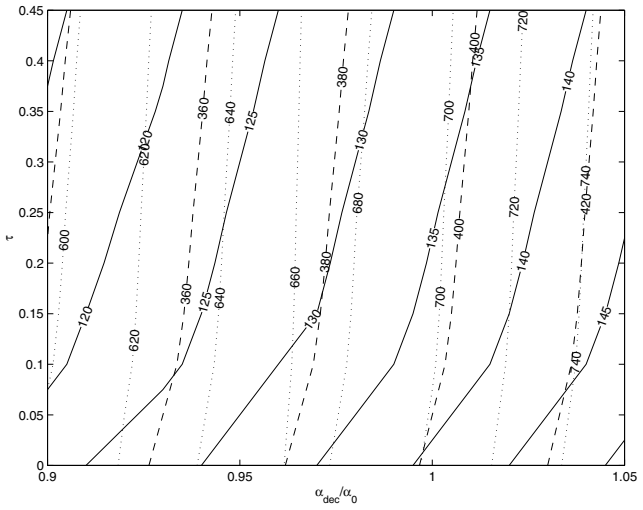

Figure 2. The separation in ℓ between the re-ionization bump and the first (solid lines), second (dashed) and third (dotted) peaks in the polarization spectrum, as a function of α at decoupling and τ. A (somewhat idealized) description of how α and τ can be measured using CMB polarization.

redshifts), when α, if varying, is much closer to the value of the present day. If the value of α at low redshift is different from that at decoupling, the peaks in the polarization power spectrum at small angular scales will be shifted sideways, while the re-ionization bump on large angular scales will not (lower right panel). It follows that by measuring the separation between the normal peaks and the bump, one can measure both α and τ, as illustrated in Fig. 2. Thus we expect that the existence of an early re-ionization epoch will, when more accurate CMB polarization data is available, lead to considerably tighter constraints on α.

A possible concern with the interpretation of our results is related to the implicit assumption of a sharp transition on the value of α happening sometime between recombination and the epoch of re-ionization. Hence, it is crucial to understand if this is a valid approximation. Apart from the value of α at the time of recombination, the knowledge of its value at two other epochs is relevant as far as the CMB anisotropies are concerned. One such epoch is the period just before recombination, which is very important for the damping of CMB anisotropies on small angular scales. The other period is the epoch of re-ionization. In this work we effectively assume that α is equal to $\alpha_{\rm rec}$ before recombination and to α_0 at the re-ionization epoch.

A value of α different from α_0 at the epoch of re-ionization will affect the CMB anisotropies through a change in the optical depth τ, once a single cosmological model is assumed. However, it is also well known that τ is itself dependent on the cosmological model through its cosmological parameters ($\Omega_{\rm m}$ and Ω_Λ for example) as well as on the cosmological density perturbations (in our case through the initial power spectrum; Avelino & Liddle 2004). The exact dependence is difficult to determine because there are several astrophysical uncertainties related to a number of relevant non-linear physical processes, which affect the accuracy of re-ionization models. In general, this problem is solved by treating τ as a free parameter (independent of the other cosmological parameters and initial power spectrum), which accounts for the relatively poor knowledge of the dependence of τ on the cosmological model and in our case on the uncertainty about the exact value of α during the re-ionization epoch. Hence, we find that, provided we treat τ as a free parameter, the lack of a precise knowledge of the value of α during the epoch of re-ionization will not affect our results. In the present work, we assume that the Universe was completely re-ionized in a relatively small redshift interval (sudden re-ionization). A more refined modelling of the re-ionization history is not yet required by *WMAP* data, but will be necessary at noise levels appropriate for *Planck* and beyond (Bruscoli, Ferrara & Scannapieco 2002; Holder et al. 2003; Hu & Holder 2003; Kaplinghat et al. 2003). On the more practical side, there are of course observational constraints on the value of α at redshifts of a few (Webb et al. 2001, 2003; Murphy et al. 2003), indicating that at that epoch the possible changes relative to the present day are already very small (and would not be detectable, on their own, through the CMB as a result of cosmic variance).

The knowledge of the value of α before recombination is also crucial for the details of the damping of small-scale CMB anisotropies. Let us assume that the variation of α around the time of recombination is given by some functional, f:

$$\frac{\alpha}{\alpha_{\rm rec}} = f\left(\frac{1+z}{1+z_{\rm rec}}\right).$$

One can determine the dependence of the Silk damping scale (Kolb & Turner 1993)

$$R_S = \left(\int_0^{t_{\rm dec}(\alpha)} {\rm d}t\, \frac{\lambda_\gamma(\alpha)}{R^2(t)}\right)^{1/2}$$

(where, λ_γ is the photon mean free path) on this functional f and determine $\alpha_{\rm eff}$ (relevant for the damping of CMB anisotropies) as the constant value of α that gives the same Silk damping scale as the variable one. Even though we did not treat $\alpha_{\rm eff}$ as another parameter in the present investigation (this will be done in future work) we expect that our constraints on $\alpha_{\rm rec}$ should also be valid (to a good approximation) for $\alpha_{\rm eff}$. This means that we are already able to constrain a combination of both α and f at the time of recombination. Also, we see that we may be able to rule out particular models for the time variation of α on the basis of the details of such variation, even if the value of α at the time of recombination is not ruled out by our analysis.

Finally, we must emphasize that the effects discussed above are direct effects of an α variation and that indirect effects are usually present as well because any variation of α is necessarily coupled with the dynamics of the Universe (Mota & Barrow 2004). In this paper we take a pragmatic approach and say that, because the CMB is quite insensitive to the details of α variations from decoupling to the present day, we do not in fact need to specify a redshift dependence for this variation: although we could have specified one if we so chose.

The price to pay would be that, because this coupling is very dependent on the particular model we consider, we would end up with very model-dependent constraints. Therefore, at this stage, and given the lack of detailed and well-motivated cosmological models for α variations, we prefer to focus on model-independent constraints and hence do not attempt to include this extra degree of freedom in our analysis. Nevertheless, given some model-independent constraints one can always translate them into constraints on the parameters of one's favourite model. In fact, we expect that some models will be ruled out on the basis of the indirect effect of a variation of α on the dynamics of the Universe rather than the direct effects we described above. This is actually a simpler case in which only the modifications to the background evolution [$a(t)$] would need to be taken into account in order to test the model, with the direct effects of a varying α being negligible.

We conclude this section by emphasizing that although a more detailed analysis taking into account the expected variation of α with time (and its direct and indirect implications for CMB anisotropies) for specific models is certainly possible, our more general work can easily be used to impose very strong constraints to more complex varying α theories once the relevant variables are computed.

4 UP-TO-DATE CMB CONSTRAINTS ON α WITH *WMAP*

We compare the recent *WMAP* temperature and cross-polarization data set with a set of flat cosmological models adopting the likelihood estimator method described in Verde et al. (2003). We restrict the analysis to flat universes. The models are computed through a modified version of the CMBFAST code with parameters sampled as follows: physical density in cold dark matter $0.05 < \Omega_c h^2 < 0.20$ (step 0.01), physical density in baryons $0.010 < \Omega_b h^2 < 0.028$ (step 0.001), $0.500 < \Omega_\Lambda < 0.950$ (step 0.025), $00.900 < \alpha_{\rm dec}/\alpha_0 < 1.050$ (step 0.005). Here h is the Hubble parameter today, $H_0 \equiv 100\,h$ km s^{-1} Mpc^{-1} (determined by the flatness condition once the above parameters are fixed), while $\alpha_{\rm dec}$ (α_0) is the value of the fine-structure constant at decoupling (today). We also vary the optical depth τ in the range 0.06–0.30 (step 0.02), the scalar spectral index of primordial fluctuations $0.880 < n_s < 1.08$ (step 0.005) and its running $-0.15 < {\rm d}n_s/{\rm d}\ln k < 0.05$ (step 0.01) both evaluated at $k_0 = 0.002$ Mpc^{-1}. We do not consider gravity waves or isocurvature modes because these further modifications are not required by the *WMAP* data (see e.g. Spergel et al. 2003). A different model for the dark energy from a cosmological constant could also change our results, but again, is not suggested by the *WMAP* data (see e.g. Melchiorri et al. 2003). An extra background of relativistic particles is also well constrained by big bang nucleosynthesis (see e.g. Bean, Hansen & Melchiorri 2001) and it will not be considered here.

The likelihood distribution function for $\alpha_{\rm dec}/\alpha_0$, obtained after marginalization over the remaining parameters, is plotted in Fig. 3. We found at 95 per cent confidence level that $0.95 < \alpha_{\rm dec}/\alpha_0 < 1.02$, improving previous bounds, (see Martins et al. 2002) based on CMB and complementary data sets. Setting ${\rm d}n_S/{\rm d}\ln k = 0$, yields $0.94 < \alpha_{\rm dec}/\alpha_0 < 1.01$ as already reported in (see Martins et al. 2004).

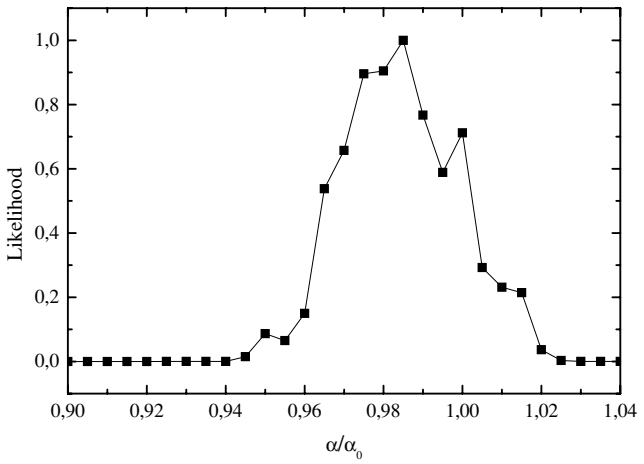

Figure 3. Likelihood distribution function for variations in the fine-structure constant obtained by an analysis of the *WMAP* data ($TT + TE$, 1 yr).

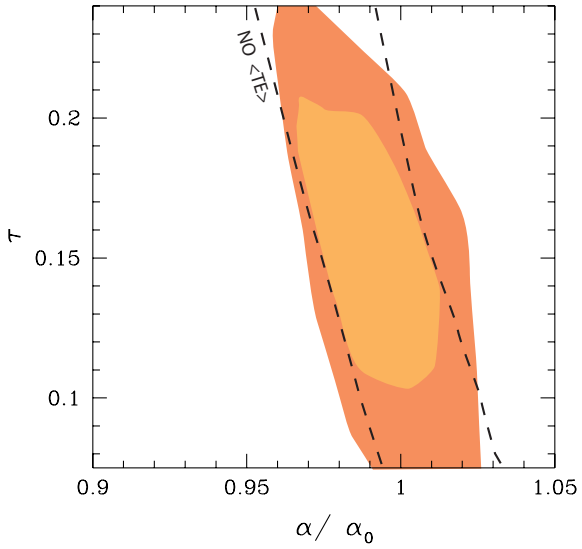

Figure 4. 2D likelihood contour plot in the α/α_0 versus τ plane for two analyses: $\langle TT\rangle$ only and $\langle TT\rangle + \langle TE\rangle$. As we can see, the inclusion of polarization data breaks the degeneracy between these two parameters.

It is interesting to consider the correlations between an α/α_0 and the other parameters in order to see how this modification to the standard model can change our conclusions about cosmology.

In Fig. 4 we plot the 2D likelihood contours in the α/α_0 versus the optical depth τ for two different analyses: using the temperature-only *WMAP* data and including the $\langle TE\rangle$ cross-spectrum temperature-polarization data. As we can see, there is a clear degeneracy between these two parameters if one considers just the $\langle TT\rangle$ spectrum: increasing the optical depth, allows for a higher value of the spectral index n_S and a lower value of α/α_0 (again, see Martins et al. 2002). As we can see from Fig. 4, the inclusion of the $\langle TE\rangle$ data, is already able to partially break the degeneracy between τ and α/α_0. However, as we explain below, more detailed measurements of the polarization spectra are needed to fully break this degeneracy.

One of the most unexpected results from the *WMAP* data is the hint for a scale-dependence of the spectral index n_S (see e.g. Kinney et al. 2003; Peiris et al. 2003). Such dependence is not predicted to be detectable in most of the viable single field inflationary model and, if confirmed, will therefore have strong consequences on the possibilities of reconstructing the inflationary potential. In Fig. 5 we plot a 2D likelihood contour in the α/α_0 versus ${\rm d}n_S/{\rm d}\ln k$ plane. As we can see, a lower value of α/α_0 makes a value of ${\rm d}n_S/{\rm d}\ln k \sim 0$ more compatible with the data. As already noticed in Bean, Melchiorri & Silk (2003), a modification of the recombination scheme can therefore provide a possible explanation for the high value of ${\rm d}n_S/{\rm d}\ln k$ compatible with the *WMAP* data.

5 FISHER MATRIX ANALYSIS SETUP

In our previous work (Martins et al. 2002), a Fisher matrix analysis was carried out, using only the CMB temperature, in order to estimate the precision with which cosmological parameters can be reconstructed in future experiments. Here, we extend this analysis by including also E-polarization measurements as well as the TE cross-correlation. We consider the planned *Planck* satellite [high frequency instrument (HFI) only] and an ideal experiment that would measure both temperature and polarization to the cosmic variance

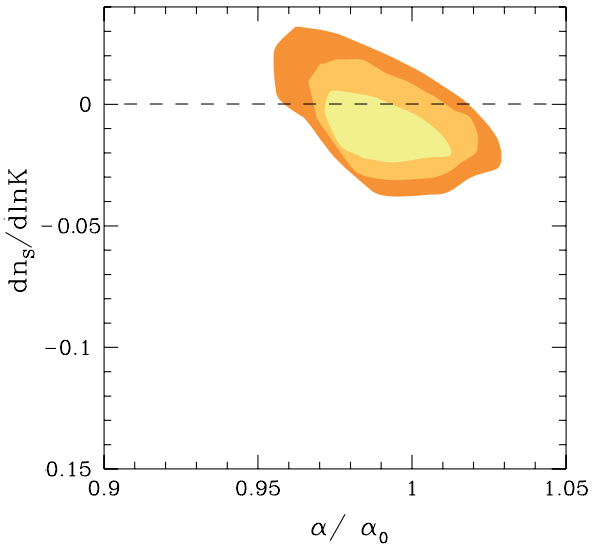

Figure 5. 2D likelihood contour plot in the α/α_0 versus $\mathrm{d}n_S/\mathrm{d}\ln k$ plane ($\langle TT\rangle + \langle TE\rangle$, 1 yr). A zero scale dependence, as expected in most of the inflationary models, is more consistent with a value of $\alpha/\alpha_0 < 1$.

limit (in the following, CVL experiment) for a range of multipoles, l, up to 2000. For illustration purposes, and particularly as a way of checking that our method is producing credible results, we will also present the Fisher Matrix Analysis (FMA) for *WMAP* and compare the corresponding predictions with existing results.

The Fisher matrix is a measure of the width and shape of the likelihood around its maximum and as such can also provide useful insight into the degeneracies among different parameters, with minimal computational effort. For a review of this technique, see Fisher (1935), Knox (1995), Jungman et al. (1996a), Jungman et al. (1996b), Bond, Efstathiou & Tegmark (1997), Tegmark, Taylor & Heavens (1997), Zaldarriaga, Spergel & Seljak (1997), Efstathiou & Bond (1999) and Efstathiou (2002). In what follows we will present a brief description of our analysis procedure, emphasizing the aspects that are new. We refer the reader to our previous work (Martins et al. 2002) for further details.

We will assume that cosmological models are characterized by the 8D parameter set

$$\Theta = \left(\Omega_{\rm b}h^2, \Omega_{\rm m}h^2, \Omega_\Lambda h^2, \mathcal{R}, n_s, Q, \tau, \alpha\right), \qquad (1)$$

where $\Omega_{\rm m} = \Omega_{\rm c} + \Omega_{\rm b}$ is the energy density in matter, Ω_Λ is the energy density due to a cosmological constant and h is a dependent variable that denotes the Hubble parameter today, $H_0 \equiv 100\ h$ km s^{-1} Mpc^{-1}. The quantity $\mathcal{R} \equiv \ell_{\rm ref}/\ell$ is the shift parameter (see Melchiorri & Griffiths 2001; Bowen et al. 2002 and references therein), which gives the position of the acoustic peaks with respect to a flat, $\Omega_\Lambda = 0$ reference model. Inclusion of the shift parameter $\mathcal{R}$ into our set of parameters takes into account the geometrical degeneracy between Ω_Λ and $\omega_{\rm m}$ (Efstathiou & Bond 1999). With our choice of the parameter set, $\mathcal{R}$ is an independent variable, while the Hubble parameter h becomes a dependent one.

n_s is the scalar spectral index and $Q = \langle \ell(\ell+1)C_\ell\rangle^{1/2}$ denotes the overall normalization, where the mean is taken over the multipole range $2 \leqslant \ell \leqslant 2000$.

We assume purely adiabatic initial conditions and we do not allow for a tensor contribution. In the FMA approach, the likelihood distribution $\mathcal{L}$ for the parameter $\boldsymbol{\Theta}$ is expanded to quadratic order around its maximum $\mathcal{L}_m$. We denote this maximum likelihood (ML) point by Θ_0 and call the corresponding model our ML model, with parameters $\omega_{\rm b} = 0.0200$, $\omega_{\rm m} = 0.1310$, $\omega_\Lambda = 0.2957$ (and $h = 0.65$), $\mathcal{R} = 0.9815$, $n_s = 1.00$, $Q = 1.00$, $\tau = 0.20$ and $\alpha/\alpha_0 = 1.00$. For the value of $z_{\rm dec}$ (which is weakly dependent on $\omega_{\rm b}$ and $\omega_{\rm tot}$) we have used the fitting formula from Hu & Sugiyama (1995). For the ML model we have $z_{\rm dec} = 1115.52$.

As mentioned above we also present the FMA for the *WMAP* best-fitting model as the fiducial model (i.e. $\omega_{\rm b} = 0.0200$, $\omega_{\rm m} = 0.1267$, $\omega_\Lambda = 0.2957$, $\mathcal{R} = 0.9636$, $n_s = 0.99$, $Q = 1.00$, $\tau = 0.17$ and $\alpha/\alpha_0 = 1.00$). Note that we will discuss cases with and without re-ionization (in the latter case $\tau = 0.0$) as well as with and without varying α.

To compute the derivatives of the power spectrum with respect to a particular cosmological parameter, one varies the considered parameter and keeps fixed the value of the others to their ML value. In particular, given that we are not constraining our analysis to the case of a flat universe, a variation in $\mathcal{R}$ is considered with all the other parameters fixed and equal to their ML value. Therefore such variation implies a variation of the dependent parameter h.

In our previous work (Martins et al. 2002), we assumed a flat fiducial model and differentiating around it requires computing open and closed models, which are calculated using different numerical techniques. We have found that this can limit the accuracy of the FMA. Here, we instead differentiate around a slightly closed model (as preferred by *WMAP*) with $\Omega_{\rm tot} = 1.01$ to avoid extra sources of numerical inaccuracies. We refer to Martins et al. (2002) for a detailed description of the numerical technique used. The experimental parameters used for the *Planck* analysis are in Table 1. Note that we use the first three channels of the *Planck* HFI only. Adding the three channels of the *Planck* low frequency instrument (LFI) leaves the expected errors unchanged: therefore they can be used for other important tasks such as foreground removal and various consistency checks, leaving the HFI channels for direct cosmological use. For the CVL experiment, we set the experimental noise to zero and we use a total sky coverage $f_{\rm sky} = 1.00$. Although this is never to be achieved in practice, the CVL experiment illustrates the precision that can be obtained in principle from CMB temperature and E-polarization measurements.

If the errors $\Theta - \Theta_0$ about the ML model are small, a quadratic expansion around this ML leads to the expression,

$$\mathcal{L} \approx \mathcal{L}_{\rm m} \exp\left[-\frac{1}{2}\sum_{ij} F_{ij}\delta\Theta_i\delta\Theta_j\right], \qquad (2)$$

where F_{ij} is the Fisher matrix, given by derivatives of the CMB power spectrum with respect to the parameters $\boldsymbol{\Theta}$.

In Martins et al. (2002) we computed the Fisher information matrix using temperature information alone. In this case for each l a derivative of the temperature power spectrum with respect to the

Table 1. Experimental parameters for *WMAP* and *Planck* (nominal mission). Note that we express the sensitivities in μK.

	WMAP			*Planck*		
ν (GHz)	40	60	90	100	143	217
$\theta_{\rm c}$ (arcmin)	31.8	21.0	13.8	10.7	8.0	5.5
$\sigma_{{\rm c}T}$ (μK)	19.8	30.0	45.6	5.4	6.0	13.1
$\sigma_{{\rm c}E}$ (μK)	28.02	42.43	64.56	*n/a*	11.4	26.7
$w^{-1}{}_{\rm c} \times 10^{15}$ (K^2 ster)	33.6	33.6	33.6	0.215	0.158	0.350
$\ell_{\rm c}$	254	385	586	757	1012	1472
$\ell_{\rm max}$		1000			2000	
$f_{\rm sky}$		0.80			0.80	

parameter under consideration is computed and then summed over all l, weighted by $\mathrm{Cov}^{-1}(\hat{C}_{Tl}^2) = \Delta C_\ell^2$. In the more general case with polarization information included, instead of a single derivative we have a vector of four derivatives with the weighting given by the the inverse of the covariance matrix (Zaldarriaga & Seljak 1997),

$$F_{ij} = \sum_l \sum_{X,Y} \frac{\partial \hat{C}_{Xl}}{\partial \Theta_i} \mathrm{Cov}^{-1}(\hat{C}_{Xl}\hat{C}_{Yl}) \frac{\partial \hat{C}_{Yl}}{\partial \Theta_j}, \quad (3)$$

where F_{ij} is the Fisher information or curvature matrix as above, Cov^{-1} is the inverse of the covariance matrix, Θ_i is the cosmological parameter we want to estimate and X, Y stands for T (temperature), E, B (polarization modes), or C (cross-correlation of the power spectra for T and E). For each l one has to invert the covariance matrix and sum over X and Y.

For Gaussian fluctuations, the covariance matrix is then given by the inverse of the Fisher matrix, $\mathbf{C} = \mathbf{F}^{-1}$ (Bond et al. 1997). The 1σ error on the parameter Θ_i with all other parameters marginalized is then given by $\sqrt{C_{ii}}$. If all other parameters are held fixed to their ML values, the standard deviation on parameter Θ_i reduces to $\sqrt{1/F_{ii}}$ (conditional value). Other cases, in which some of the parameters are held fixed and others are being marginalized over can easily be worked out.

In the case in which all parameters are being estimated jointly, the joint error on parameter i is given by the projection on the ith coordinate axis of the multidimensional hyper-ellipse, which contains a fraction γ of the joint likelihood. The equation of the hyper-ellipse is

$$(\mathbf{\Theta} - \mathbf{\Theta}_0)\mathbf{F}(\mathbf{\Theta} - \mathbf{\Theta}_0)^t = q_{1-\gamma}, \quad (4)$$

where $q_{1-\gamma}$ is the quantile for the probability $1 - \gamma$ for a χ^2 distribution with 6, 7 and 8 degrees of freedom. For $\gamma = 0.683$ (1σ confidence level) we have for 6, 7 and 8 degrees of freedom, $q_{1-\gamma} = 7.03$, $q_{1-\gamma} = 8.18$ and $q_{1-\gamma} = 9.30$, respectively.

As observed in Martins et al. (2002) the accuracy with which parameters can be determined depends on their true value as well as on the number of parameters considered. Note that the FMA assumes that the values of the parameters of the true model are in the vicinity of $\mathbf{\Theta}_0$. The validity of the results therefore depends on this assumption, as well as on the assumption that $a_{\ell m}$ is an independent Gaussian random variable. If the FMA predicted errors are small enough, the method is self-consistent and we can expect the FMA prediction to reproduce in a correct way the exact behaviour. This is indeed the case for the present analysis, with the notable exception of ω_Λ, which as expected suffers from the geometrical degeneracy.

Also, special care must be taken when computing the derivatives of the power spectrum with respect to the cosmological parameters. This differentiation strongly amplifies any numerical errors in the spectra, leading to larger derivatives, which would artificially break degeneracies among parameters. In the present work we implement double-sided derivatives, which reduce the truncation error from second-order to third-order terms. The choice of the step size is a trade-off between truncation error and numerical inaccuracy dominated cases. For an estimated numerical precision of the computed models of order 10^{-4}, the step size should be approximately 5 per cent of the parameter value (Press et al. 1992), though it turns out that for derivatives in direction of α and n_s the step size can be chosen to be as small as 0.1 per cent. After several tests, we have chosen step sizes varying from 1 to 5 per cent for ω_b, ω_m, ω_Λ and $\mathcal{R}$. This choice gives derivatives with an accuracy of approximately 0.5 per cent. The derivatives with respect to Q are exact, being the power spectrum itself.

6 FMA WITHOUT RE-IONIZATION

We will now start to describe the results of our analysis in detail. In order to avoid confusion, we will begin in this section by describing the results for the case $\tau = 0$ (because most of the crucial degeneracies can be understood in this case) and leave the more relevant case of non-zero τ for the following section. While it may seem pointless after *WMAP* to discuss the cases without (or with very little) re-ionization, we shall see that a lot can be learned by comparing the results for the various cases.

6.1 Analysis results: the FMA forecast

Tables 2 and 3 summarize the results of our FMA for *WMAP*, *Planck* and a CVL experiment. We consider the cases of models with and without a varying α being included in the analysis, for $\tau = 0$. We also consider the use of temperature information alone (TT), E-polarization alone (EE) and both channels ($EE + TT$) jointly.

Table 2 shows the 1σ errors on each of the parameters of our FMA for a standard model, that is with no re-ionization or variation of α. The inclusion of polarization data does indeed increase the accuracy on each parameter for *Planck* and for a CVL experiment. For the *Planck* mission, the polarization data helps to better constrain each of the parameters though the increase in accuracy is only of the order 10 per cent in most cases. The error in ω_Λ is still large and larger than those of the other parameters. Indeed, this error is almost insensitive to the experimental details when only temperature is considered in the analysis, which of course is a manifestation of the so-called geometrical degeneracy (Efstathiou & Bond 1999; Efstathiou 2002).

The existence of this nearly exact degeneracy limits in a fundamental way the accuracy on measurements of the Hubble constant as well as of the curvature of the Universe obtained with the CMB observations and hence limits the accuracy on ω_m and ω_Λ. This degeneracy can only be removed when constraints on the geometry of the Universe from other complementary observations, such as Type Ia supernova or gravitational lensing, are jointly considered (Efstathiou & Bond 1999; Efstathiou 2002). Our plots show that actually using polarization data the confidence contours can narrow significantly on the ω_Λ axis. This case is very different from other degeneracies between parameters, which actually can be broken with good enough CMB data and by probing a larger set of angular scales, i.e. an enlarged range of multipoles l, as well as using the CMB polarized data.

The geometrical degeneracy gives rise to almost identical CMB anisotropies in universes with different background geometries but identical matter content, lines of constant $\mathcal{R}$ are directions of degeneracy. This degeneracy along $\delta(\omega_\mathrm{m}^{-1/2}\mathcal{R}) = 0$ results in a linear relation between $\delta\omega_\mathrm{k}$ and $\delta\omega_\Lambda$, with coefficients that depend on the fiducial model.

This is why we used the $\mathcal{R}$ parameter to replace ω_k in our Fisher analysis instead of the ω_D parameter of Efstathiou & Bond (1999) and Efstathiou (2002).

The accuracy on the parameter $\mathcal{R}$ is related to the ability of fixing the positions of the Doppler peaks. Hence *Planck* is expected to determine $\mathcal{R}$ with high accuracy given that it samples the Doppler peak region almost entirely. Indeed this is the case with the error reducing from 4 per cent for *WMAP* to 1 per cent for *Planck* and to 0.5 per cent for a CVL experiment (see Table 2).

Table 3 shows the 1σ errors on each of the parameters of our FMA for a model with a time-varying α. While the inclusion of a varying α as a parameter (with the nominal value equal to that

Table 2. Fisher matrix analysis results for standard model: expected 1σ errors for the *WMAP* and *Planck* satellites as well as for a CVL experiment. The columns are: marg. (the error with all other parameters being marginalized over), fixed (the other parameters are held fixed at their ML value) and joint (all parameters being estimated jointly.

Quantity	1σ errors (per cent)								
	WMAP			*Planck* HFI			CVL		
	Marg.	Fixed	Joint	Marg.	Fixed	Joint	Marg.	Fixed	Joint
				Polarization					
$\omega_{\rm b}$	1437.41	52.93	4111.09	6.40	0.99	18.31	0.48	0.25	1.38
$\omega_{\rm m}$	619.43	31.47	1771.62	3.57	0.33	10.22	0.70	0.03	2.01
ω_Λ	1397.45	980.08	3996.79	38.76	34.40	110.84	11.28	9.94	32.27
n_s	260.43	33.68	744.83	1.47	0.91	4.20	0.30	0.08	0.86
$\mathcal{Q}$	474.57	25.13	1357.31	2.21	0.45	6.32	0.24	0.07	0.68
$\mathcal{R}$	666.04	22.10	1904.92	3.53	0.30	10.09	0.66	0.03	1.88
				Temperature					
$\omega_{\rm b}$	2.79	1.26	7.97	0.82	0.59	2.36	0.55	0.38	1.59
$\omega_{\rm m}$	4.58	0.83	13.11	1.44	0.12	4.12	1.09	0.08	3.11
ω_Λ	115.59	86.53	330.59	91.65	86.37	262.11	80.68	77.25	230.74
n_s	1.50	0.52	4.30	0.48	0.13	1.36	0.33	0.07	0.96
$\mathcal{Q}$	0.80	0.34	2.29	0.19	0.10	0.55	0.17	0.07	0.48
$\mathcal{R}$	4.17	0.73	11.92	1.41	0.11	4.03	1.05	0.07	2.99
				Temperature and polarization					
$\omega_{\rm b}$	2.78	1.26	7.95	0.77	0.51	2.20	0.32	0.21	0.91
$\omega_{\rm m}$	4.56	0.83	13.05	1.16	0.12	3.32	0.55	0.03	1.58
ω_Λ	114.34	86.09	327.03	31.79	31.72	90.92	9.87	9.49	28.24
n_s	1.50	0.52	4.28	0.39	0.13	1.12	0.20	0.06	0.57
$\mathcal{Q}$	0.80	0.34	2.28	0.18	0.10	0.52	0.14	0.05	0.40
$\mathcal{R}$	4.15	0.73	11.86	1.14	0.10	3.25	0.52	0.03	1.49

Table 3. Fisher matrix analysis results for a model with a varying α: expected 1σ errors for the *WMAP* and *Planck* satellites as well as for a CVL experiment. The columns are: marg. (the error with all other parameters being marginalized over), fixed (the other parameters are held fixed at their ML value) and joint (all parameters are being estimated jointly).

Quantity	1σ errors (per cent)								
	WMAP			*Planck* HFI			CVL		
	Marg.	Fixed	Joint	Marg.	Fixed	Joint	Marg.	Fixed	Joint
				Polarization					
$\omega_{\rm b}$	4109.93	52.93	11754.68	6.42	0.99	18.36	1.10	0.25	3.16
$\omega_{\rm m}$	844.65	31.47	2415.75	7.14	0.33	20.43	1.64	0.03	4.69
ω_Λ	1483.80	980.08	4243.77	41.78	34.40	119.50	12.03	9.94	34.41
n_s	365.06	33.68	1044.09	3.90	0.91	11.16	0.79	0.08	2.25
$\mathcal{Q}$	2415.47	25.13	6908.40	3.24	0.45	9.28	0.24	0.07	0.69
$\mathcal{R}$	4847.40	22.10	13863.91	10.13	0.30	28.98	1.19	0.03	3.39
α	887.24	3.51	2537.58	2.62	0.05	7.50	0.40	<0.01	1.15
				Temperature					
$\omega_{\rm b}$	10.41	1.26	29.78	0.97	0.59	2.78	0.77	0.38	2.21
$\omega_{\rm m}$	8.51	0.83	24.34	2.54	0.12	7.27	2.04	0.08	5.85
ω_Λ	125.00	86.53	357.51	107.64	86.37	307.85	93.06	77.25	266.16
n_s	3.05	0.52	8.73	1.32	0.13	3.76	1.04	0.07	2.97
$\mathcal{Q}$	2.11	0.34	6.05	0.20	0.10	0.57	0.17	0.07	0.50
$\mathcal{R}$	21.12	0.73	60.40	1.50	0.11	4.29	1.06	0.07	3.02
α	4.64	0.12	13.27	0.43	0.02	1.22	0.31	0.01	0.88
				Temperature and polarization					
$\omega_{\rm b}$	10.00	1.26	28.60	0.87	0.51	2.49	0.38	0.21	1.09
$\omega_{\rm m}$	8.23	0.83	23.54	1.61	0.12	4.60	0.67	0.03	1.90
ω_Λ	123.13	86.09	352.17	31.79	31.72	90.92	9.96	9.49	28.49
n_s	2.97	0.52	8.48	0.85	0.13	2.44	0.32	0.06	0.91
$\mathcal{Q}$	2.04	0.34	5.82	0.18	0.10	0.53	0.14	0.05	0.41
$\mathcal{R}$	20.34	0.73	58.18	1.36	0.10	3.88	0.60	0.03	1.72
α	4.46	0.12	12.75	0.31	0.02	0.88	0.11	<0.01	0.32

of the standard model) has no noticeable effect on the accuracy of the other parameters for a CVL experiment, for *Planck* and most notoriously for *WMAP* this is not the case (compare Table 2 with Table 3). For these two satellite missions the accuracy of most of the other parameters is reduced by inclusion of this extra parameter as should be expected (for allowing an extra degree of freedom). The same trend as before is observed with the inclusion of polarization data.

From our *WMAP* predictions one would expect to be able to constrain α to approximately 5 per cent accuracy at 1 σ, while the actual analysis presented in previous section gives an accuracy of the order of 7 per cent at 2σ. This is in reasonable agreement with our prediction with the discrepancy being a result of the effect of a $\tau \neq 0$ (see next section). On the other hand, the results of our forecast are that *Planck* and a CVL experiment will be able to constrain variations in α with an accuracy of 0.3 and 0.1 per cent, respectively (1σ confidence level, all other parameters marginalized). If all parameters are being estimated simultaneously, then these limits increase to approximately 0.9 and 0.3 per cent, respectively. This is therefore the best that one can hope to do with the CMB alone: it is somewhat below the 10^{-5} level of the claimed detection of a variation using quasar absorption systems (Webb et al. 2001, 2003; Murphy et al. 2003), but it is also at a much higher redshift, where any variations relative to the present day are expected to be larger than at $z \sim 3$. Therefore, for specific models such limits can be at least as constraining as those at low redshift. On the other hand, there is a way of improving this, which is to combine CMB data with other observables: this is the approach we already took in Avelino et al. (2001) and Martins et al. (2002), for example.

From these tables we conclude that for *WMAP* the inclusion of polarization information does not improve significantly the accuracy on each of the parameters, because its accuracy from polarization data alone is expected to be worse than that from temperature alone by a factor of $\simeq 10^2$–10^3. With *Planck* though there is room for improvement, with the accuracy from polarization alone at most only a factor 10 poorer than from temperature. Also, for this case a better accuracy on ω_Λ is obtained using polarization data alone versus using temperature data alone, for both cases with and without inclusion of a varying α. For the CVL experiment the polarization makes a real difference, with the accuracy of polarization alone being slightly better than that of the temperature alone. Combining the two typically increases the accuracy on most parameters by a factor of order 2. As expected this is most noticeably so for ω_Λ. Assuming that the improvement was only owing to the use of independent sets of data, we should expect an improvement by at least a factor of $\sqrt{2}$.

6.2 Analysis results: confidence contours

In order to provide better intuition for the various effects involved, we show in Figs 6 and 7 joint 2D confidence contours for all pairs of parameters (all remaining parameters marginalized) for the cases shown in Tables 2 and 3, respectively (i.e. the cases $\tau = 0$ without and with a varying α). For each case, we show plots corresponding to our three experiments (*WMAP*, *Planck* and CVL) and contours for TT only, EE only and all combined. Note that all contours are 2σ. To notice that in the *WMAP* case the errors from E only are very large, hence the contours for T coincide almost exactly with the temperature-polarization combined case. In the CVL case, it is the E contours that almost coincide with the combined ones.

Again, starting with the standard model in Fig. 6 we can observe the expected degeneracies between parameters, as previously discussed in Efstathiou & Bond (1999) and Efstathiou (2002). These degeneracies among parameters limit our ability to disentangle one parameter from another, using CMB observations alone. The search for means to break such degeneracies is therefore of extreme importance.

The contour plots for *WMAP* exhibit the degeneracy directions in the planes $(\omega_\Lambda, \mathcal{R})$, $(n_s, \mathcal{R})$, for example $\mathcal{R}$ suffers strong degeneracy with $\omega_\mathrm{m}, \omega_\Lambda$. A correlation between ω_Λ and both n_s and Q is also noticeable. The contour plot in the plane $(\omega_\Lambda, \mathcal{R})$ prevents a good constraint of both parameters in agreement with results tabulated in Table 2. For both *Planck* and a CVL experiment, the direction of degeneracy for polarization alone is almost orthogonal to this direction while the direction for temperature alone corresponds to $\mathcal{R} =$ constant. The degeneracy direction on the $(\omega_\mathrm{m}, \mathcal{R})$ plane is defined by $\delta(\omega_\mathrm{m}^{1/2}\mathcal{R}) = 0$.

The contour plots for *Planck* are perhaps the perfect example of a case where the degeneracy directions between $\mathcal{R}$ and ω_Λ are different and almost orthogonal for temperature and polarization alone. This therefore explains why the joint use of T and E data helps to break degeneracies. For example the degeneracy between $\mathcal{R}$ and ω_b present when polarization is considered alone, disappears when temperature information is included. It is interesting to notice, when comparing *WMAP* and *Planck* plots, that the joint use of T and E does not necessarily break degeneracies between the parameters, whilst narrowing down the width of the contour plots without affecting the degeneracy directions.

For the CVL experiment the effect of polarization is to better constrain all parameters in particular ω_Λ, helping to narrow down the range of allowed values in the ω_Λ direction as compared with temperature alone. For instance in the plane (n_s, ω_Λ) the direction n_s is well constrained but there is no discriminatory power on the ω_Λ direction until polarization data is included. For all but the 2D planes containing ω_Λ, the contours are narrowed to give better constraints to each of the parameters. This is a result of the exact degeneracy mentioned above: more accurate CMB measurements simply narrow the likelihood contours around the degeneracy lines on the $(\omega_\Lambda, \omega_k)$ plane (Efstathiou & Bond 1999; Efstathiou 2002).

Fig. 6 also shows that ω_b and ω_m are slightly anticorrelated for the *Planck* experiment. For the *WMAP* experiment the plot shows a degeneracy between ω_m and ω_Λ. If we restrict ourselves to spatially flat models, there is a relationship between these two parameters that will result in similar position of the Doppler peaks. The degeneracy direction can be obtained by differentiating l_D, the location of the maximum of the first Doppler peak (Efstathiou & Bond 1999; Efstathiou 2002) These degeneracy lines in the $\omega_\mathrm{c} - \omega_\Lambda$ plane are given by (assuming that ω_b is held fixed in the expression of l_D):

$$\omega_\mathrm{c} = (\omega_\mathrm{c})_t + b\omega_\Lambda; \qquad b = -\frac{(\partial l_\mathrm{D}/\partial\omega_\Lambda)_t}{(\partial l_\mathrm{D}/\partial\omega_\mathrm{c})_t}. \tag{5}$$

Unlike the geometrical degeneracy, this is not exact. Both the height and the amplitude of the peaks depend upon the parameter ω_m, hence an experiment such as *Planck*, which probes high multipoles, will be able to break this degeneracy. This is clearly visible in Fig. 6 for both *Planck* and a CVL experiment (compare with the case for *WMAP*).

Similarly the condition of constant height of the first Doppler peak determines the degeneracies among ω_b, ω_c, n_s and Q. Both *WMAP* and *Planck* are sensitive to higher multipoles than the first Doppler peak. The other peaks help to pin down the value of ω_b and therefore these degeneracies can actually be broken. The plots for *WMAP* show a mild degeneracy in the (n_s, ω_b) plane for the

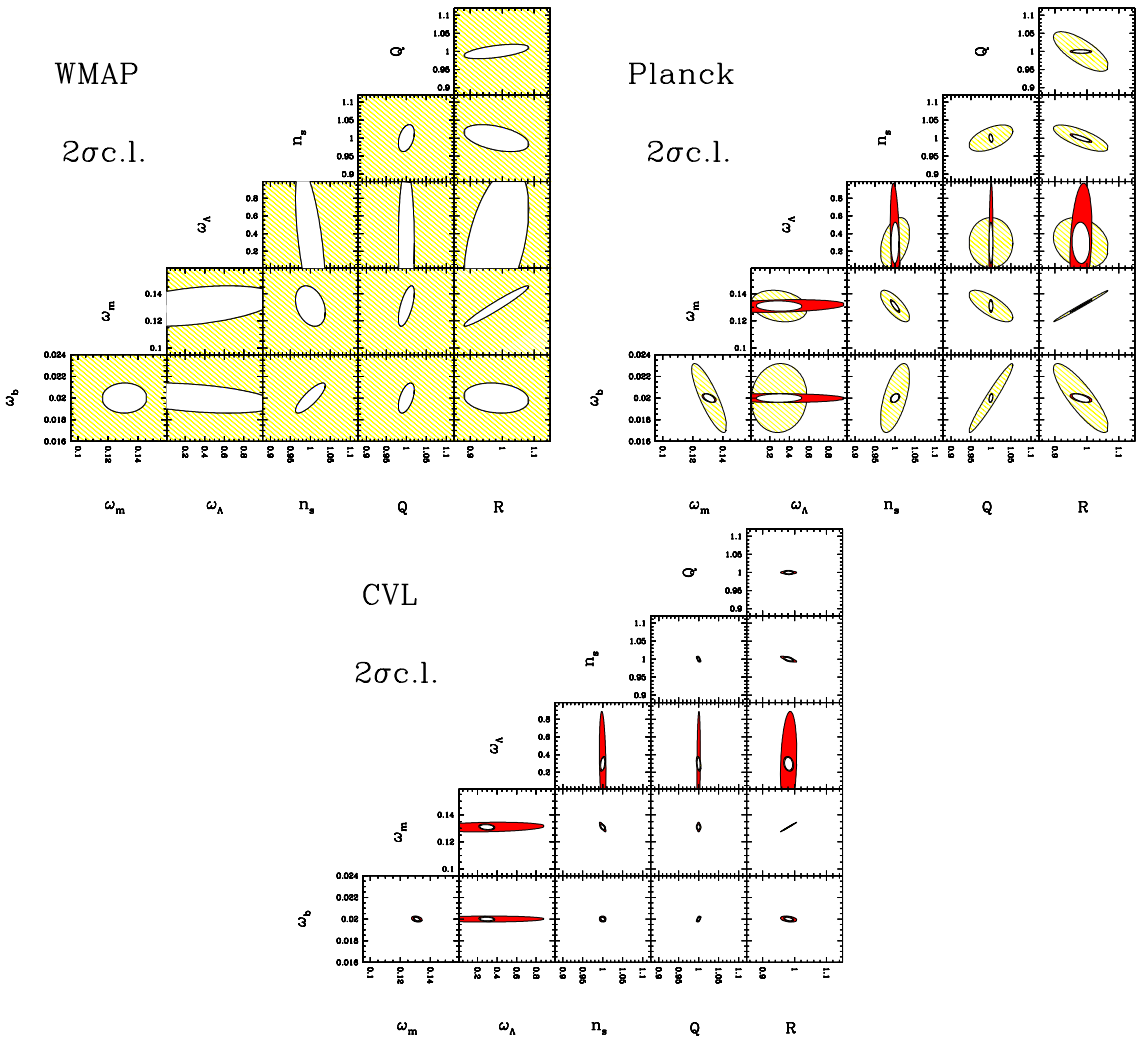

Figure 6. (This figure appears in colour in the online version of the journal on *Synergy*.) Ellipses containing 95.4 per cent (2σ) of joint confidence (all other parameters marginalized) using temperature alone (red), E-polarization alone (yellow) and both jointly (white), for a standard model. In the *WMAP* case, the errors from E only are very large, hence the contours for T coincide almost exactly with the temperature–polarization combined case. In the CVL case, it is the E contours that almost coincide with the combined ones.

EE + *TT* joint analysis, which seems to be lifted for the *Planck* experiment.

In our previous works (Avelino et al. 2000, 2001; Martins et al. 2002), we observed a degeneracy between α and some of the other parameters, most notably $\omega_{\rm b}$, n_s and $\mathcal{R}$. Our previous FMA analysis with temperature information alone (Martins et al. 2002) showed that these degeneracies could be removed by using higher multipole measurements, e.g. from *Planck*. The question we want to address here is whether the use of polarization data allows further improvements.

As previously pointed out, a variation in α affects both the location and height of the Doppler peaks, hence this parameter will be correlated with parameters that determine the peak structure. Therefore, from the previous discussion on degeneracies among parameters for a standard model, one can anticipate the degeneracies exhibited in Fig. 7 in the planes (α, n_s), $(\alpha, \mathcal{R})$, (α, Q), $(\alpha, \omega_{\rm b})$ and $(\alpha, \omega_{\rm m})$.

In our previous work (Martins et al. 2002), we showed that using temperature alone the degeneracies of α with $\omega_{\rm b}$ and α with n_s are lifted as we move from *WMAP* to *Planck* when higher multipoles measurements can break it.

All the degeneracy directions for these pairs of parameters for the *WMAP* joint analysis (which actually is dominated by the temperature data alone) are approximately preserved by using polarization data alone for the *Planck* experiment. A joint analysis of temperature and polarization helps to narrow down the confidence contours without necessarily breaking the degeneracy.

With the inclusion of the new parameter α, the *WMAP* contour plots get wider as compared with Fig. 6, while leaving almost unchanged the degeneracy directions in most planes of pairs of parameters. For *Planck*, the contour plots are still wider whilst the degeneracy directions for polarization alone change for some of the parameters. For example, the direction of degeneracy between the $(\mathcal{R}, n_s)$ changes when compared with Fig. 6, which is a result of the presence of the degeneracy between α and n_s, which is almost orthogonal to the direction of degeneracy in the plane $(\alpha, \omega_{\rm m})$. Another changed direction of degeneracy is that of $(\omega_{\rm b}, \mathcal{R})$, with wider contour plots. The degeneracy present in the *WMAP* plot for the plane $(\alpha, \omega_{\rm b})$ seems to be broken with *Planck* data. Notice the strong degeneracy between α and $\mathcal{R}$ that still persists when using jointly temperature and polarization data.

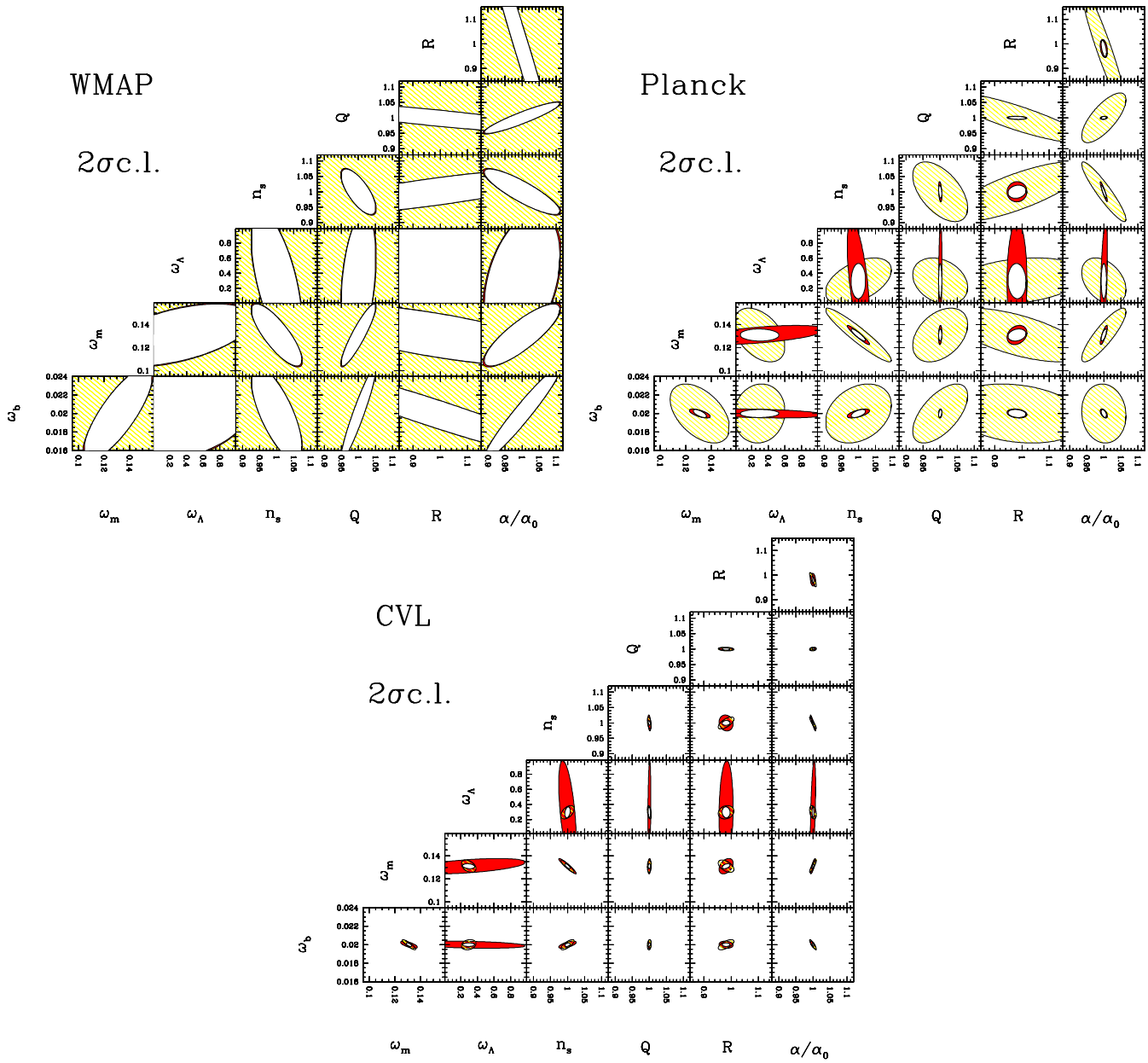

Figure 7. (This figure appears in colour in the online version of the journal on *Synergy*.) Ellipses containing 95.4 per cent (2σ) of joint confidence (all other parameters marginalized) using temperature alone (red), E-polarization alone (yellow) and both jointly (white), for a model with varying α. In the *WMAP* case, the errors from E only are very large, hence the contours for T coincide almost exactly with the temperature–polarization combined case. In the CVL case, it is the E contours that almost coincide with the combined ones.

Using temperature and polarization data jointly seems either to help to break some of the degeneracies or at least to narrow down the contours without lifting the degeneracy, in particular for those cases where the degeneracy directions for each of the temperature and polarization are different (in some cases almost orthogonal, see for example the planes containing ω_Λ as one of the parameters).

For the CVL experiment, most of the plots remain unchanged when compared with no inclusion of α, with the temperature alone contour plot slightly wider in the (n_s, ω_Λ) plane. A large range of possibilities along the ω_Λ direction still remains, as expected from the exact geometrical degeneracy mentioned above.

7 FMA WITH RE-IONIZATION

The existence of a period when the intergalactic medium was re-ionized as well as its driving mechanism are still to be understood. One possible way of studying this phase is via the CMB polarization anisotropy. The optical depth to electrons of the CMB photons enhances the polarization signal at large angular scales (see Fig. 1) introducing a bump in the polarization spectrum at small multipoles. On the other hand, re-ionization decreases the amplitude of the acoustic peaks on the temperature power spectrum at intermediate and small angular scales. This signal has now been detected

by *WMAP* via the temperature polarization cross power-spectrum Kogut et al. (2003).

In the absence of polarization observations, the optical depth to Thomson scattering is degenerate with the amplitude of the fluctuations, Q (with $Q\mathrm{e}^{\tau} = \text{constant}$). From previous Fisher matrix analyses for a standard model, e.g. Zaldarriaga et al. (1997), one expects that the inclusion of polarization measurements will help to better constrain some of the cosmological parameters, by probing the ionization history of the Universe, hence constraining τ and breaking degeneracies of this with other parameters. We will now repeat the analysis of the previous section for the case $\tau \neq 0$.

7.1 Analysis results: the FMA forecast

Tables 4 and 5 summarize the results of our FMA for *WMAP*, *Planck* and a CVL experiment. We consider the cases of models with and without a varying α being included in the analysis and also two values of the optical depth, $\tau = 0.2$ (close to the one preferred by *WMAP*) and $\tau = 0.02$. We also consider the use of temperature information alone (*TT*), E-polarization alone (*EE*) and both channels (*EE* + *TT*) jointly. To show that our FMA fiducial model is close enough to the *WMAP* best-fitting model to produce similar FMA results, we display in Table 6 the results of our FMA using as a fiducial model the *WMAP* best-fitting model.

For the sake of completeness we also consider the case *TE* by including the results for *EE* + *TT* + *TE* as well as *EE* + *TE* for 4-yr *WMAP*. Tables 7 and 8 displays the results of our FMA for 4-yr *WMAP* using the *WMAP* fiducial model. The FMA predictions for 4-yr *WMAP* are to be compared with the recent *WMAP* 1-yr results.

The errors in most of the other cosmological parameters are unaffected by the presence of re-ionization if one has both temperature and polarization data. If one has just one of them then the accuracy is quite different and also it will depend on whether one has high or low τ. This is because different degeneracies may be dominant in each case, while combining temperature and polarization information helps break such degeneracies.

The inclusion of the new parameter τ for a standard model reduces the accuracy in other parameters for all but the CVL experiment (and in this case for all but ω_Λ) as can be seen from a comparison of Table 4 with Table 2.

Comparing the case $\tau = 0.20$ to that of $\tau = 0.02$, an immediate effect of considering a large value of τ is to increase the accuracy on τ itself. For example the case with temperature and polarization information used jointly, the accuracy on the other parameters is not necessarily reduced by considering a larger value of τ while its accuracy remains almost the same for a CVL experiment. Whilst the effect of a large value of τ, considering the case of temperature and polarization used jointly, for *WMAP* is to increase the accuracy on most of the parameters particularly noticeable for the parameters α and τ; for *Planck* only the accuracy on τ is improved while the other parameters have slightly worse accuracy; finally for a CVL experiment the accuracy is the same for all but ω_Λ, which is slightly worse, and τ, which is much better. It is interesting to note that while for *WMAP* a large value of τ does indeed help to improve the accuracy on most parameters, for *Planck* and a CVL experiment the accuracy is improved using polarization data alone but the inverse is true using temperature data alone. Hence it is not surprising the results obtained when one considers temperature and polarization jointly.

Table 4. Fisher matrix analysis results for a standard model with inclusion of re-ionization ($\tau = 0.20$): expected 1σ errors for the *WMAP* and *Planck* satellites as well as for a CVL experiment. The columns are: marg. (the error with all other parameters being marginalized over), fixed (the other parameters are held fixed at their ML value) and joint (all parameters are being estimated jointly).

Quantity	1σ errors (per cent)								
	WMAP			*Planck* HFI			CVL		
	Marg.	Fixed	Joint	Marg.	Fixed	Joint	Marg.	Fixed	Joint
				Polarization					
ω_b	223.67	22.18	639.70	6.21	1.11	17.75	0.48	0.25	1.38
ω_m	104.48	22.12	298.81	3.37	0.39	9.64	0.70	0.03	1.99
ω_Λ	1231.56	113.78	3522.35	37.37	22.87	106.89	11.40	9.99	32.61
n_s	107.77	5.31	308.22	1.53	0.96	4.38	0.30	0.08	0.86
Q	139.04	18.38	397.68	2.23	0.51	6.38	0.24	0.07	0.67
$\mathcal{R}$	91.43	20.44	261.50	3.33	0.35	9.52	0.65	0.03	1.86
τ	156.71	9.64	448.22	5.74	2.78	16.42	1.81	1.52	5.18
				Temperature					
ω_b	10.59	1.35	30.28	0.86	0.60	2.46	0.57	0.38	1.64
ω_m	13.54	0.88	38.72	1.51	0.13	4.31	1.10	0.08	3.14
ω_Λ	114.06	96.36	326.22	110.15	96.15	315.03	98.15	86.00	280.72
n_s	8.64	0.53	24.72	0.54	0.13	1.56	0.36	0.07	1.04
Q	1.46	0.36	4.19	0.20	0.11	0.56	0.17	0.07	0.50
$\mathcal{R}$	13.98	0.78	39.98	1.47	0.12	4.21	1.05	0.07	3.01
τ	107.58	13.26	307.68	16.50	8.28	47.20	14.02	5.89	40.09
				Temperature and polarization					
ω_b	3.10	1.34	8.86	0.80	0.53	2.30	0.32	0.21	0.92
ω_m	5.09	0.88	14.56	1.24	0.12	3.55	0.55	0.03	1.58
ω_Λ	89.62	72.75	256.33	30.58	22.04	87.46	10.72	9.85	30.65
n_s	1.66	0.52	4.76	0.43	0.13	1.23	0.20	0.05	0.58
Q	0.96	0.36	2.74	0.19	0.10	0.53	0.14	0.05	0.41
$\mathcal{R}$	4.49	0.78	12.85	1.22	0.11	3.48	0.52	0.03	1.49
τ	12.38	7.90	35.41	4.04	2.65	11.56	1.73	1.48	4.96

Table 5. Fisher matrix analysis results for a model with varying α and inclusion of re-ionization ($\tau = 0.20$): expected 1σ errors for the *WMAP* and *Planck* satellites as well as for a CVL experiment. The columns are: marg. (the error with all other parameters being marginalized over), fixed (the other parameters are held fixed at their ML value) and joint (all parameters are being estimated jointly).

Quantity	1σ errors (per cent)								
	WMAP			*Planck* HFI			CVL		
	Marg.	Fixed	Joint	Marg.	Fixed	Joint	Marg.	Fixed	Joint
					Polarization				
$\omega_{\rm b}$	281.91	22.18	806.27	6.46	1.11	18.47	1.09	0.25	3.12
$\omega_{\rm m}$	446.89	22.12	1278.15	7.75	0.39	22.17	1.61	0.03	4.60
ω_Λ	1248.94	113.78	3572.04	41.61	22.87	119.01	11.60	9.99	33.17
n_s	126.90	5.31	362.93	4.14	0.96	11.85	0.77	0.08	2.22
Q	200.97	18.38	574.78	2.99	0.51	8.55	0.24	0.07	0.68
$\mathcal{R}$	254.76	20.44	728.63	9.56	0.35	27.33	1.19	0.03	3.40
α	111.52	3.74	318.96	2.66	0.06	7.62	0.40	<0.01	1.14
τ	275.13	9.64	786.88	8.81	2.78	25.19	2.26	1.52	6.45
					Temperature				
$\omega_{\rm b}$	13.56	1.35	38.78	1.09	0.60	3.12	0.83	0.38	2.37
$\omega_{\rm m}$	17.73	0.88	50.71	3.76	0.13	10.74	2.64	0.08	7.55
ω_Λ	137.68	96.36	393.77	111.61	96.15	319.21	98.97	86.00	283.05
n_s	10.10	0.53	28.88	2.18	0.13	6.24	1.49	0.07	4.26
Q	2.41	0.36	6.89	0.20	0.11	0.57	0.18	0.07	0.50
$\mathcal{R}$	23.86	0.78	68.25	1.58	0.12	4.53	1.06	0.07	3.04
α	5.16	0.13	14.76	0.66	0.02	1.88	0.41	0.01	1.18
τ	111.97	13.26	320.24	26.93	8.28	77.02	20.32	5.89	58.11
					Temperature and polarization				
$\omega_{\rm b}$	7.37	1.34	21.07	0.91	0.53	2.61	0.38	0.21	1.09
$\omega_{\rm m}$	6.94	0.88	19.85	1.81	0.12	5.17	0.67	0.03	1.91
ω_Λ	89.69	72.75	256.51	30.89	22.04	88.36	10.79	9.85	30.85
n_s	2.32	0.52	6.65	0.97	0.13	2.77	0.33	0.05	0.93
Q	1.63	0.36	4.67	0.19	0.10	0.54	0.14	0.05	0.41
$\mathcal{R}$	14.22	0.78	40.68	1.43	0.11	4.08	0.60	0.03	1.72
α	3.03	0.13	8.68	0.34	0.02	0.97	0.11	<0.01	0.32
τ	12.67	7.90	36.23	4.48	2.65	12.80	1.80	1.48	5.15

As we go from Tables 6 to 8 the accuracy on all parameters increases as should be expected. For the 4-yr *WMAP* one predicts an accuracy of 3 and 11 per cent on α and τ, respectively, as opposed to 4 and 14 per cent, respectively, for the 2-yr mission.

The results of our forecast are that *WMAP* (2-yr mission) is able to constrain τ with accuracy of the order 13 per cent, which is approximately two times better than the current precision obtained from the *WMAP* 1-yr observations, of the order of 23 per cent. While our FMA predictions for 4-yr *WMAP*, gives an accuracy of the order 10 per cent using all temperature, polarization and temperature-polarization ($TT + EE + TE$) cross correlation information.

Planck and a CVL experiment can constrain α with accuracies of the order 0.3 and 0.1 per cent, respectively, and τ with accuracies of the order 4.5 and 1.8 per cent, respectively.

For *WMAP*, the accuracy on τ from polarization data alone is worse by a factor of 2 than from temperature alone. On the other hand, for *Planck* and the CVL experiment the accuracy from polarization is better by a factor of 3 and 8, respectively, than from temperature alone. While the accuracy on α from polarization alone is worse by a factor of the order 22 and 4 than from temperature alone for *WMAP* and *Planck*, respectively. For a CVL experiment the accuracies are similar for both polarization and temperature data alone.

The accuracy on τ obtained with *Planck* using temperature data alone is roughly the same as a CVL experiment. This suggests that *Planck* is indeed a CVL experiment with respect to temperature. With the inclusion of polarization the accuracy for the CVL experiment is improved by a factor of 4 when compared to *Planck* satellite.

7.2 Analysis results: confidence contours

As before, we show in Figs 8–10 all joint 2D confidence contours (all remaining parameters marginalized).

From Fig. 8 without α, we can infer a good agreement between our predictions and *WMAP* observations. Particularly striking is the good agreement for the contour plots in the (n_s,τ) plane, which clearly exhibits the observed degeneracy (Spergel et al. 2003). For *Planck*, the inclusion of polarization data helps to break degeneracies in particular between τ and the other parameters, for example with n_s. For a CVL experiment, the contours are further narrowed with the joint temperature polarization analysis in agreement with the tabulated accuracies on τ.

Again, looking at Fig. 10 with α, our predictions for the contour plots in the plane (τ, n_s) are in close agreement with the observed degeneracy (Verde et al. 2003). This same plot shows that the degeneracy direction between α and n_s is almost orthogonal to that between τ and n_s, The net result of this is a better accuracy on α when the parameter τ is included (compare Tables 3 and 5) while the accuracy on τ itself remains almost unchanged with inclusion of α (compare Tables 4 and 5). This is in agreement with our

Table 6. Fisher matrix analysis results for a model with varying α and inclusion of re-ionization (for *WMAP* best-fitting model as the Fisher analysis fiducial model, $\tau = 0.17$): expected 1σ errors for the *WMAP* and *Planck* satellites as well as for a CVL experiment. The columns are: marg. (the error with all other parameters being marginalized over), fixed (the other parameters are held fixed at their ML value) and joint (all parameters are being estimated jointly).

Quantity	1σ errors (per cent)								
	WMAP			*Planck* HFI			CVL		
	Marg.	Fixed	Joint	Marg.	Fixed	Joint	Marg.	Fixed	Joint
					Polarization				
$\omega_{\rm b}$	285.33	26.18	816.08	5.84	0.87	16.70	0.96	0.12	2.73
$\omega_{\rm m}$	445.06	28.16	1272.90	7.48	0.46	21.41	1.40	0.03	4.00
ω_Λ	184.17	144.61	3386.80	44.12	24.08	126.18	12.83	9.33	36.70
n_s	161.11	6.14	460.78	4.22	1.00	12.08	0.71	0.08	2.04
Q	191.24	21.06	546.95	2.91	0.55	8.32	0.25	0.07	0.73
R	221.83	21.69	634.44	8.81	0.35	25.19	0.79	0.02	2.26
α	113.11	4.52	323.49	2.61	0.07	7.48	0.32	<0.01	0.91
τ	336.62	11.25	962.75	9.25	3.05	26.45	2.32	1.30	6.63
					Temperature				
$\omega_{\rm b}$	18.50	0.98	52.91	0.98	0.35	2.80	0.73	0.24	2.08
$\omega_{\rm m}$	17.89	0.94	51.17	3.30	0.14	9.45	2.31	0.08	6.60
ω_Λ	149.92	83.49	428.77	107.48	83.30	307.39	94.61	74.50	270.59
n_s	9.50	0.54	27.17	2.07	0.14	5.91	1.42	0.07	4.06
Q	3.27	0.37	9.36	0.21	0.11	0.60	0.19	0.07	0.53
R	34.95	0.72	99.97	1.34	0.10	3.84	0.86	0.06	2.45
α	7.95	0.13	22.75	0.59	0.02	1.69	0.37	0.01	1.06
τ	119.62	17.00	342.11	32.86	9.93	93.98	25.31	6.84	72.38
					Temperature and polarization				
$\omega_{\rm b}$	9.15	0.98	26.18	0.84	0.32	2.39	0.37	0.11	1.07
$\omega_{\rm m}$	7.55	0.94	21.58	1.62	0.13	4.65	0.61	0.03	1.75
ω_Λ	95.34	71.51	272.68	32.24	22.94	92.22	11.80	9.21	33.76
n_s	2.58	0.54	7.39	0.93	0.14	2.67	0.33	0.05	0.94
Q	1.77	0.37	5.06	0.19	0.11	0.56	0.15	0.05	0.43
R	17.55	0.71	50.19	1.19	0.10	3.42	0.49	0.02	1.40
α	3.89	0.13	11.12	0.31	0.02	0.88	0.10	<0.01	0.30
τ	13.57	9.49	38.81	4.71	2.92	13.48	1.81	1.28	5.18

Table 7. Fisher matrix analysis results for a standard model with inclusion of re-ionization (for *WMAP* best-fitting model as the Fisher analysis fiducial model, $\tau = 0.17$): expected 1σ errors for the *WMAP*4-yr experiment. The columns are: marg. (the error with all other parameters being marginalized over), fixed (the other parameters are held fixed at their ML value) and joint (all parameters are being estimated jointly).

Quantity	1σ errors (per cent) 4-yr *WMAP*					
	Marg.	Fixed	Joint	Marg.	Fixed	Joint
	Polarization (*EE*)			Temperature (*TT*)		
$\omega_{\rm b}$	110.64	16.58	316.44	7.33	0.81	20.96
$\omega_{\rm m}$	49.48	17.16	141.52	8.91	0.77	25.49
ω_Λ	622.34	97.58	1779.93	113.30	83.39	324.06
n_s	69.43	4.89	198.58	6.68	0.53	19.11
Q	79.22	13.51	226.58	0.90	0.32	2.58
R	46.52	13.04	133.06	9.25	0.59	26.47
τ	100.84	8.21	288.40	102.72	16.70	293.79
	Temp. + Pol. (*TT* + *EE*)			All (*TT* + *EE* + *TE*)		
$\omega_{\rm b}$	2.14	0.80	6.11	2.13	0.80	6.08
$\omega_{\rm m}$	3.09	0.77	8.85	3.08	0.77	8.81
ω_Λ	90.70	63.84	259.41	86.97	62.69	248.75
n_s	1.46	0.52	4.18	1.45	0.52	4.15
Q	0.52	0.32	1.48	0.52	0.32	1.48
R	2.86	0.59	8.17	2.84	0.59	8.12
τ	10.52	7.45	30.08	10.41	7.44	29.78

discussion in Section 3 and quantitatively explains why our α mechanism (summarized in Fig. 2) works. The accuracy on n_s is similar to that obtained without τ (compare Tables 3 and 5) but gets worse with inclusion of α (compare Tables 4 and 5).

In other words, the inclusion of re-ionization helps to lift most of the degeneracies when using information from both the temperature and polarization jointly, hence increasing the accuracies for the cases of interest, i.e. α and τ.

7.3 The α–τ degeneracy

Our results clearly indicate a crucial degeneracy between α and τ. In order to study it in more detail, we have extracted the relevant results from Table 5 and Fig. 10 and re-displayed them in Table 9 and Fig. 11. Both of these summarize the forecasts for the precision in determining both parameters with *Planck* and the CVL experiment.

It is apparent from Fig. 11 that *TT* and *EE* suffer from degeneracies in different directions, for the reasons explained above. Thus combining high-precision temperature and polarization measurements one can most effectively constrain both variations of α and τ. *Planck* will be essentially CVL for temperature but there will still be considerable room for improvement in polarization. This therefore argues for a post-*Planck* polarization-dedicated experiment, not least because polarization is, in itself, better at determining cosmological parameters than temperature.

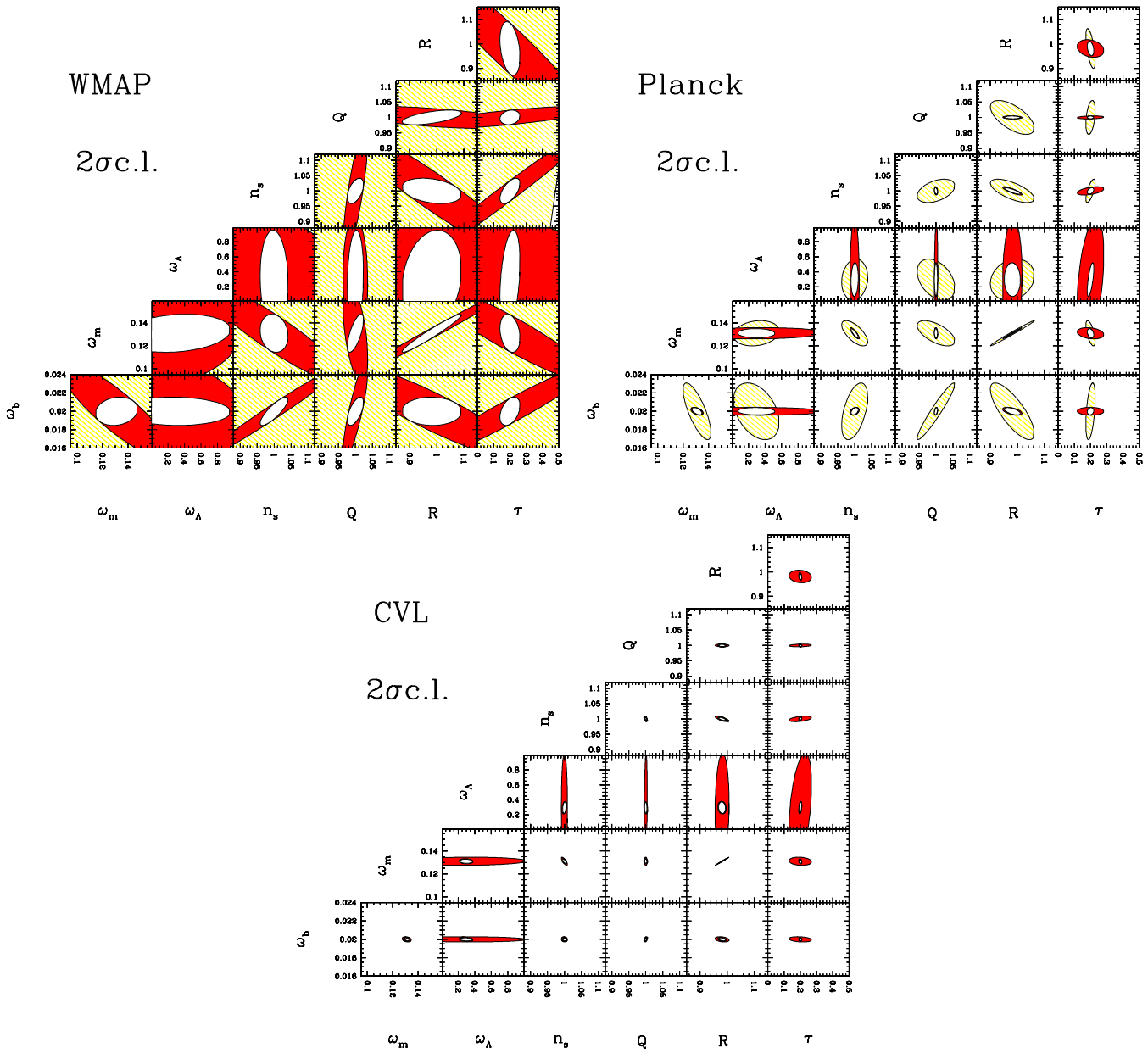

Figure 8. (This figure appears in colour in the online version of the journal on *Synergy*.) Ellipses containing 95.4 per cent (2σ) of joint confidence (all other parameters marginalized) using temperature alone (red), E-polarization alone (yellow) and both jointly (white), for a standard model with inclusion of re-ionization ($\tau = 0.20$).

We conclude that *Planck* data alone will be able to constrain variations of α at the epoch of decoupling with 0.34 per cent accuracy (1σ, all other parameters marginalized), which corresponds to approximately a factor 5 improvement on the current upper bound. On the other hand, the CMB alone can only constrain variations of α up to $\mathcal{O}(10^{-3})$ at $z \sim 1100$. Going beyond this limit will require additional (non-CMB) priors on some of the other cosmological parameters. This result is to be contrasted with the variation measured in quasar absorption systems by Webb et al. (2001), $\delta\alpha/\alpha_0 = \mathcal{O}(10^{-5})$ at $z \sim 2$. Nevertheless, there are models where deviations from the present value could be detected using the CMB.

8 CONCLUSIONS

We have presented a detailed analysis of the current *WMAP* constraints on the value of the fine-structure constant α at decoupling. We have found that current constraints on α, coming from *WMAP* alone, are as strong as all previously existing cosmological constraints (CMB combined with additional data, e.g. coming from Type Ia supernovae or the *HST* Key project) put together. On the other hand, we have also shown that the CMB alone can determine α to a maximum accuracy of 0.1 per cent: one can only improve on this number by again combining CMB data with other observables.

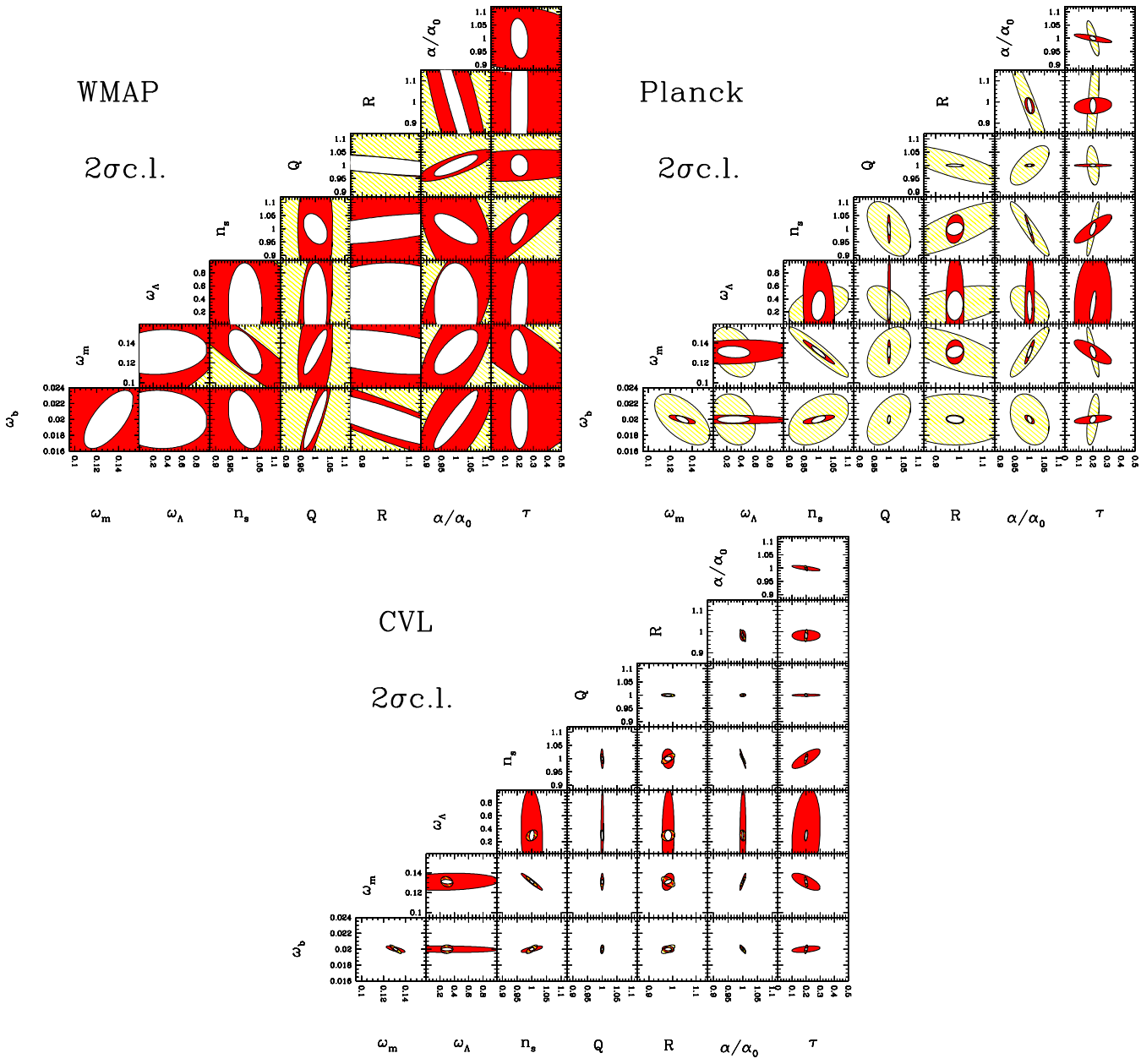

Figure 9. (This figure appears in colour in the online version of the journal on *Synergy*.) Ellipses containing 95.4 per cent (2σ) of joint confidence (all other parameters marginalized) using temperature alone (red), E-polarization alone (yellow) and both jointly (white), for a model with varying α and inclusion of re-ionization ($\tau = 0.20$).

Note that such combination of data sets is not without its subtleties: see Martins et al. (2002) for a discussion of some specific issues related to this case.

Hence, this accuracy is well below the 10^{-5} detection of Webb et al. (2001). However, one must keep in mind that one is dealing with much higher redshifts (approximately 1000 rather than a few). Given that in the simplest, best motivated models for α variation, one expects it to be a non-decreasing function of time, one finds that a constraint of 10^{-3} at the epoch of decoupling can be as constraining for these models as the Webb et al. results. In addition, there are also constraints on variations of α at the epoch of nucleosynthesis, which are at the level of 10^{-2} (Avelino et al. 2001). The main difference between them is that while CMB constraints are model independent, the big bang nucleosynthesis (BBN) ones are not (they rely on the assumption of the Gasser–Leutwyler phenomenological formula for the dependence of the neutron–proton mass difference on α).

As discussed in the main text, we focused our analysis on model independent constraints and in fact explicitly avoided discussing constraints for specific models. Nevertheless it is quite easy, given the constraints (and forecasts) presented here, to translate them into constraints for the specific free parameters of one's preferred model.

We have also presented a thorough analysis of future CMB constraints on α and the other cosmological parameters, specifically for the *WMAP* and *Planck* surveyor satellites, and compared them to those for an ideal (CVL) experiment. Comparisons with currently published (1-yr) *WMAP* data indicates that our Fisher matrix analysis pipeline is quantitatively robust and accurate.

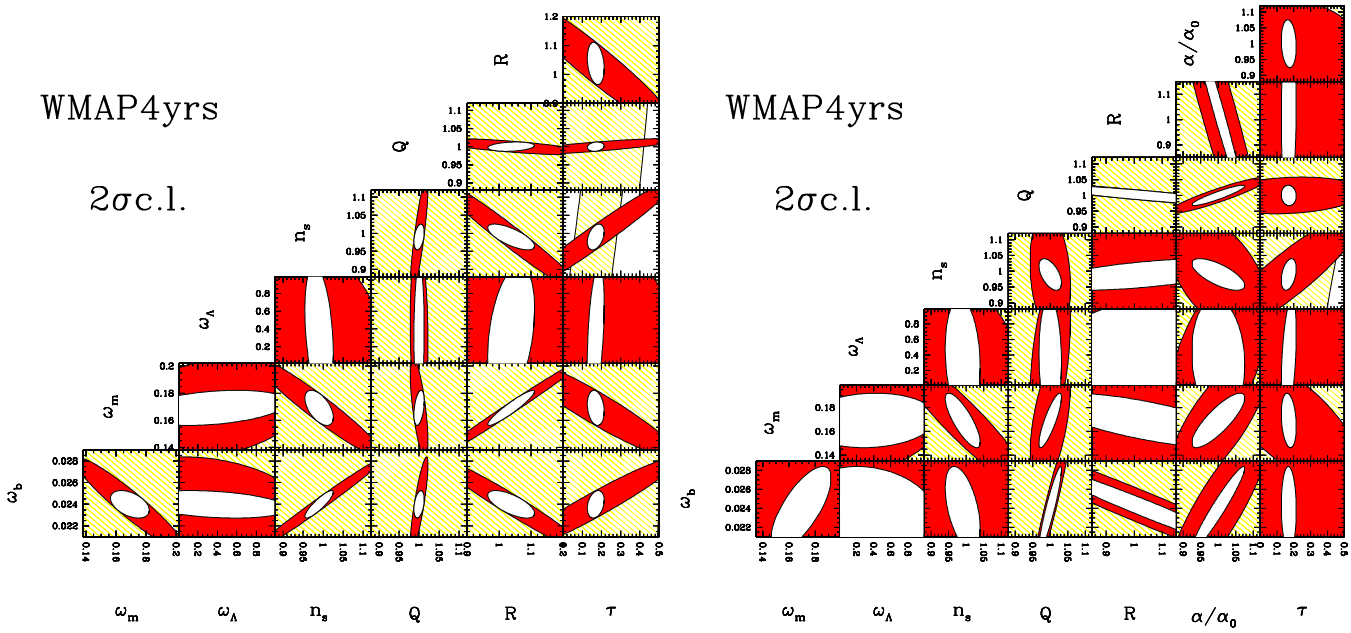

Figure 10. (This figure appears in colour in the online version of the journal on *Synergy*.) Ellipses containing 95.4 per cent (2σ) of joint confidence (all other parameters marginalized) for the 4-yr *WMAP*, using temperature alone (red), E-polarization alone (yellow) and both jointly (white).

Table 8. Fisher matrix analysis results for a model with varying α and inclusion of re-ionization (for *WMAP* best-fitting model as the Fisher analysis fiducial model, $\tau = 0.17$): expected 1σ errors for the 4-yr *WMAP* experiment. The columns are: marg. (the error with all other parameters being marginalized over), fixed (the other parameters are held fixed at their ML value) and joint (all parameters are being estimated jointly).

Quantity	1σ errors (per cent) 4-yr *WMAP*					
	Marg.	Fixed	Joint	Marg.	Fixed	Joint
	Polarization (*EE*)			Temperature (*TT*)		
ω_b	173.74	16.58	496.91	14.09	0.81	40.30
ω_m	260.62	17.16	745.40	13.76	0.77	39.36
ω_Λ	637.28	97.58	1822.66	133.73	83.39	382.47
n_s	108.18	4.89	309.41	7.86	0.53	22.47
Q	96.60	13.51	276.30	2.33	0.32	6.67
R	133.23	13.04	381.04	26.29	0.59	75.19
α	69.10	2.48	197.62	5.83	0.12	16.66
τ	228.69	8.21	654.07	103.86	16.70	297.05
	Temp. + Pol. ($TT + EE$)			All ($TT + EE + TE$)		
ω_b	7.50	0.80	21.44	7.41	0.80	21.18
ω_m	5.48	0.77	15.66	5.46	0.77	15.62
ω_Λ	91.57	63.84	261.91	87.48	62.69	250.20
n_s	2.03	0.52	5.82	2.03	0.52	5.81
Q	1.31	0.32	3.73	1.30	0.32	3.71
R	14.34	0.59	41.01	14.17	0.59	40.53
α	3.08	0.11	8.80	3.05	0.11	8.71
τ	10.65	7.45	30.46	10.52	7.44	30.08

Table 9. Fisher matrix analysis results for a model with varying α and re-ionization: expected 1σ errors for the *Planck* satellite and for the CVL experiment (see the text for details). The columns are: marg. (the error with all other parameters being marginalized over), fixed (the other parameters are held fixed at their ML value) and joint (all parameters are being estimated jointly).

	1σ errors (per cent)					
	Planck HFI			CVL		
	Marg.	Fixed	Joint	Marg.	Fixed	Joint
	E-polarization only (*EE*)					
α	2.66	0.06	7.62	0.40	<0.01	1.14
τ	8.81	2.78	25.19	2.26	1.52	6.45
	Temperature only (*TT*)					
α	0.66	0.02	1.88	0.41	0.01	1.18
τ	26.93	8.28	77.02	20.32	5.89	58.11
	Temperature + polarization ($TT + EE$)					
α	0.34	0.02	0.97	0.11	<0.01	0.32
τ	4.48	2.65	12.80	1.80	1.48	5.15

By separately studying the temperature and polarization channels, we have explicitly shown that the degeneracy directions can be quite different in the two cases and hence that by combining them many such degeneracies can be broken. We have also shown that in the ideal case CMB (EE) polarization is a much more accurate estimator of cosmological parameters than CMB temperature.

Nevertheless, polarization measurements are much harder to do in practice. For example, for the case of *WMAP* the (*EE*) channel will provide a quite modest contribution for the overall parameter estimation analysis. This situation is quite different for *Planck*: here the contributions of the temperature and polarization channels are quite similar. In fact, we have also shown that the *Planck* temperature measurements will be almost CVL, while its polarization measurements will be well below this ideal limit. (This fact was previously known, but it had never been quantified as was done in the present paper.) Hence this, together with the fact that polarization is intrinsically superior for the purpose of cosmological parameter estimation, make a strong case for a post-*Planck*, polarization-dedicated experiment.

Our analysis can readily be repeated for other experiments. It should be particularly enlightening to study cases of interferometer

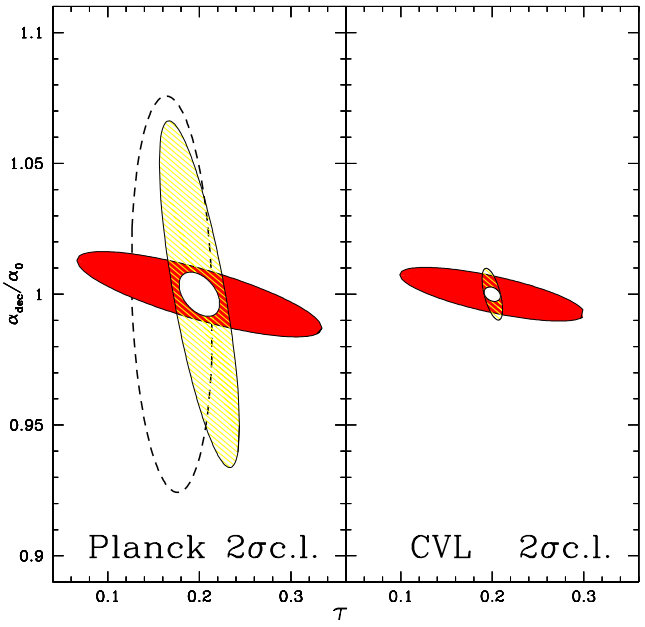

Figure 11. (This figure appears in colour in the online version of the journal on *Synergy*.) Ellipses containing 95.4 per cent (2σ) of joint confidence in the α versus τ plane (all other parameters marginalized), for the *Planck* and cosmic variance limited (CVL) experiments, using temperature alone (red), E-polarization alone (yellow) and both jointly (white). The dashed contour represents the 4-yr *WMAP* forecast using $TT + EE + TE$ jointly.

experiments and compare them with the *WMAP* and *Planck* satellites. On the other hand, it would also be possible to extend it to include gravity waves, ioscurvature modes, or a dark energy component different from a cosmological constant. However, none of these is currently required by existing (CMB and other) data and the latter two are in fact strongly constrained.

To conclude, the prospects of further constraining α at high redshift are definitely bright. In addition, further progress is expected at low redshift, where at least three (to our knowledge) independent groups are currently trying to confirm the (Webb et al. 2001, 2003; Murphy et al. 2003) claimed detection of a smaller α. All of these are using VLT data, while the original work (Webb et al. 2001, 2003; Murphy et al. 2003) used Keck data. This alone will provide an important test of the systematics of the pipeline, plus in addition the three groups are using quite different methods. These and other completely new methods that may be devised thus offer the real prospect of an accurate mapping of the cosmological evolution of the fine-structure constant, $\alpha = \alpha(z)$.

Finally, a point that we have not discussed at all for reasons of space, but that should be kept in mind in the context of forthcoming experiments, is that any time variation of α will be related (in a model-dependent way) to violations of the Einstein Equivalence principle (Will 2001). Thus a strong experimental and/or observational confirmation of either of them will have revolutionary implications not just for cosmology but for physics as a whole.

ACKNOWLEDGMENTS

The authors would like to thank Anthony Challinor and Anthony Lasenby for useful discussions and Dave Green for help with the LaTeX. GR acknowledges a Leverhulme Fellowship at the University of Cambridge, RT is partially supported by the Swiss National Science Foundation and the Schmidheiny Foundation and CJAPM is funded by FCT (Portugal), under grant FMRH/BPD/1600/2000. This work was done in the context of the European network CMB-net and was performed on COSMOS, the Origin3800 owned by the UK Computational Cosmology Consortium, supported by Silicon Graphics/Cray Research, HEFCE and PPARC.

REFERENCES

Avelino P. P., Liddle A. R., 2004, MNRAS, 348, 105
Avelino P. P., Martins C. J. A. P., Rocha G., 2000, Phys. Lett., B483, 210
Avelino P. P., Martins C. J. A. P., Rocha G., Viana P., 2000, Phys. Rev. D, 62, 123 508
Avelino P. P. et al., 2001, Phys. Rev., D, 64, 103 505
Barrow J. D., Sandvik H. B., Magueijo J., 2002, Phys. Rev. D, 65, 63 504
Battye R. A., Crittenden R., Weller J., 2001, Phys. Rev. D, 63, 43 505
Bean R., Hansen S. H., Melchiorri A., 2001, Phys. Rev. D, 64, 103 508
Bean R., Melchiorri A., Silk J., 2003, Phys. Rev. D, 68, 083501
Bennett C. L. et al., 2003, ApJS, 148, 1
Bond J. R., Efstathiou G., Tegmark M., 1997, Mon. Not. Roy. Astron. Soc., 291, L33
Bowen R., Hansen S. H., Melchiorri A., Silk J., Trotta R., 2002, MNRAS, 334, 760
Bruscoli M., Ferrara A., Scannapieco E., 2002, MNRAS, 330, L43
Challinor A., 2000, Phys. Rev. D, 62, 43 004
Damour T., 2003a, Ap&SS, 283, 445
Damour T., 2003b, in Proc. 10th Int. Workshop on Neutrino Telescopes, gr-qc/0306023
Damour T., Nordtvedt K., 1993, Phys. Rev. D, 48, 3436
Efstathiou G., 2002, MNRAS, 332, 193
Efstathiou G., Bond J. R., 1999, MNRAS, 304, 75
Fisher R., 1935, J. R. Stat. Soc., 98, 39
Fujii Y., 2003, Ap&SS, 283, 559
Hannestad S., 1999, Phys. Rev. D, 60, 23 515
Hinshaw G. et al., 2003, ApJS, 148, 135
Holder G., Haiman Z., Kaplinghat M., Knox L., 2003, ApJS, 595, 13
Hu W., 2003, Ann. Phys., 303, 203
Hu W., Holder G. P., 2003, Phys. Rev. D, 68, 23 001
Hu W., Sugiyama N., 1995, Phys. Rev. D, 51, 2599
Hu W., White M. J., 1997, New Astron., 2, 323
Ivanchik A., Petitjean P., Rodriguez E., Varshalovich D., 2003, Ap&SS, 283, 583
Jungman G., Kamionkowski M., Kosowsky A., Spergel D. N., 1996a, Phys. Rev. D, 54, 1332
Jungman G., Kamionkowski M., Kosowsky A., Spergel D. N., 1996b, Phys. Rev. Lett., 76, 1007
Kamionkowski M., Kosowsky A., Stebbins A., 1997a, Phys. Rev. Lett., 78, 2058
Kamionkowski M., Kosowsky A., Stebbins A., 1997b, Phys. Rev. D, 55, 7368
Kaplinghat M., Scherrer R. J., Turner M. S., 1999, Phys. Rev. D, 60, 23 516
Kaplinghat M., Chu, M., Haiman Z., Holder G., Knox L., Skordis C., 2003, ApJ, 583, 24
Kinney W. H., Kolb E. W., Melchiorri A., Riotto A., 2004, Phys. Rev. D, 69, 103516
Knox L., 1995, Phys. Rev. D, 52, 4307
Kogut A. et al., 2003, ApJS, 148, 161
Kolb E. W., Turner M. S., 1993, The Early Universe. Addison-Wesley Publishing Company, California
Kosowsky A., 1996, Ann. Phys., 246, 49
Kovac J., Leitch E. M., Pryke C., Carlstrom J. E., Halverson N. W., Holzapfel W. L., 2002, Nat, 420, 772
Marion H. et al., 2003, Phys. Rev. Lett., 90, 150 801
Martins C. J. A. P., 2002, Philos. Trans. R. Soc. Lond., A, 360, 2681
Martins C. J. A. P., Melchiorri A., Trotta R., Bean R., Rocha G., Avelino P. P., Viana P. T. P., 2002, Phys. Rev. D, 66, 23 505
Martins C. J. A. P., Melchiorri A., Rocha G., Trotta R., Avelino P. P., Viana P., 2004, Phys. Lett. B., 585, 29

Melchiorri A., Griffiths L. M., 2001, New Astron. Rev., 45, 321
Melchiorri A., Mersini L., Odman C. J., Trodden M., 2003, Phys. Rev. D, 68, 43 509
Mota D. F., Barrow J. D., 2004, Phys. Lett. B., 581, 141
Murphy M. T., Webb J. K., Flambaum V. V., 2003, MNRAS, 345, 609
Peiris H. V. et al., 2003, ApJS, 148, 213
Polchinski J., 1998, String Theory, VoIs 1 and 2. Cambridge Univ. Press, Cambridge
Press W. H., Vetterling W. T., Teukolsky S. A., Flannery B. P., 1992, Numerical Recipes in Fortran. Cambridge Univ. Press, Cambridge
Santiago D. I., Kalligas D., Wagoner R. V., 1998, Phys. Rev. D, 58, 124 005
Seljak U., Zaldarriaga M., 1997, Phys. Rev. Lett., 78, 2054
Sigurdson K., Kurylov A., Kamionkowski M., 2003, Phys. Rev. D, 68, 1035
Spergel D. et al., 2003, ApJS, 148, 175
Tegmark M., Taylor A., Heavens A., 1997, ApJ, 480, T22
Trotta R., Hansen S. H., 2004, Phys. Rev. D, 69, 023509
Uzan J.-P., 2003, Rev. Mod. Phys., 75, 403
Verde L. et al., 2003, ApJS, 148, 195
Webb J. K., Murphy M. T., Flambaum V. V., Dzuga V. A., Barrow J. D., Churchill C. W., Prochaska J. X., Wolfe A. M., 2001, Phys. Rev. Lett., 87, 91 301
Webb J. K., Murphy M. T., Flambaum V. V., Curran S. J., 2003, ApJS, 283, 565
Will C. M., 2001, Living Rev. Relativ., 4, 4
Zaldarriaga M., Seljak U., 1997, Phys. Rev. D, 55, 1830
Zaldarriaga M., Spergel D. N., Seljak U., 1997, ApJ, 488, 1

This paper has been typeset from a TEX/LATEX file prepared by the author.